University of Alberta

Cooperative Communication Under Adaptive Transmission

by

Tyler Nechiporenko

A thesis submitted to the Faculty of Graduate Studies and Research in partial fulfillment of the requirements for the degree of **Master of Science**.

Department of Electrical and Computer Engineering

Edmonton, Alberta
Fall 2008

Library and Archives Canada

Published Heritage Branch

395 Wellington Street
Ottawa ON K1A 0N4
Canada

Bibliothèque et Archives Canada

Direction du Patrimoine de l'édition

395, rue Wellington
Ottawa ON K1A 0N4
Canada

Your file Votre référence
ISBN: 978-0-494-47374-0
Our file Notre référence
ISBN: 978-0-494-47374-0

NOTICE:
The author has granted a non-exclusive license allowing Library and Archives Canada to reproduce, publish, archive, preserve, conserve, communicate to the public by telecommunication or on the Internet, loan, distribute and sell theses worldwide, for commercial or non-commercial purposes, in microform, paper, electronic and/or any other formats.

The author retains copyright ownership and moral rights in this thesis. Neither the thesis nor substantial extracts from it may be printed or otherwise reproduced without the author's permission.

AVIS:
L'auteur a accordé une licence non exclusive permettant à la Bibliothèque et Archives Canada de reproduire, publier, archiver, sauvegarder, conserver, transmettre au public par télécommunication ou par l'Internet, prêter, distribuer et vendre des thèses partout dans le monde, à des fins commerciales ou autres, sur support microforme, papier, électronique et/ou autres formats.

L'auteur conserve la propriété du droit d'auteur et des droits moraux qui protège cette thèse. Ni la thèse ni des extraits substantiels de celle-ci ne doivent être imprimés ou autrement reproduits sans son autorisation.

In compliance with the Canadian Privacy Act some supporting forms may have been removed from this thesis.

While these forms may be included in the document page count, their removal does not represent any loss of content from the thesis.

Conformément à la loi canadienne sur la protection de la vie privée, quelques formulaires secondaires ont été enlevés de cette thèse.

Bien que ces formulaires aient inclus dans la pagination, il n'y aura aucun contenu manquant.

Canada

Abstract

IN THIS THESIS, the use of adaptive source transmission with amplify-and-forward (AF) relaying is proposed. Three different adaptive techniques are considered: (i) optimal simultaneous power and rate adaptation; (ii) constant power with optimal rate adaptation; (iii) channel inversion with fixed rate. The capacity of these adaptive protocols are derived for the AF cooperative system over both independent and identically distributed (i.i.d.) Rayleigh fading and non-identically and independent distributed (non-i.i.d.) Rayleigh fading environments. The capacity analysis is based on an upper bound on the effective received signal-to-noise ratio (SNR), and its tightness is validated by the use of Monte Carlo simulation. The use of constant-power, fixed switching rate-adaptive M-QAM transmission is applied to AF cooperative network as a practical technique for rate adaptation. The outage probability, achievable spectral efficiency, and error rate performance are analyzed. The spectral efficiency of fixed switching rate-adaptive M-QAM is compared to the theoretical capacity of constant power with optimal rate adaptation. Optimization of the switching thresholds for constant-power, rate-adaptive five-mode M-QAM transmission for the AF cooperative network is investigated. The optimum switching levels are designed to meet a prescribed average bit error rate (BER) and compared to the previous results with fixed switching.

Acknowledgements

Numerous people have supported me during my graduate study at Alberta, and I would like to thank my family, friends, colleagues and mentors.

I would like to thank my supervisor Professor Chintha Tellambura for his continuous support during my masters program. Professor Tellambura always had an open door and never minded me barging into his office, even if it was over a dozen times in a day. Professor Tellambura has taught me a lot about wireless communication research, I appreciate his exceptionally strong knowledge in this area, and his willingness to help me which has made this research extremely successful.

I would like to thank Professor Ha Nguyen at the University of Saskatchewan, for assistance in my masters research. I owe a great deal of thanks to Professor Nguyen for his guidance during my undergraduate program at the University of Saskatchewan as he taught me a lot about wireless communication, without this initial step I don't know if my masters research would have been as successful.

Great appreciation for the funding support from NSERC for the Canada Graduate Scholarship, iCORE for the Graduate Student Scholarship, and the University of Alberta FGSR for the Walter H. Johns Graduate Fellowship. Without these funding supporters I would have never been able to complete my studies.

I would like to thank my mother, father, and brother for their love and

support during my masters program. A special thanks goes out to my mom for cooking me care packages to bring back to Edmonton every time I would go back home.

Thank you to everyone else who has helped me in someway or another.

Contents

1 Introduction **1**

1.1 Motivation 1

1.2 Contributions 3

1.3 Thesis Outline 5

2 Preliminaries and Background **7**

2.1 Cooperative Communications 7

2.1.1 Cooperative System Model 9

2.2 Adaptive Transmission 12

2.2.1 Adaptive Transmission System Model 14

2.3 Summary 17

3 Channel Capacity of Cooperative Communication Under Adaptive Transmission **18**

3.1 Introduction 18

3.2 Channel and System Model 20

3.2.1 System Model 20

3.2.2 Probability Distribution Function Derivation 22

3.3 Capacity Analysis Under Adaptive Transmission 24

3.3.1 Optimal Simultaneous Power and Rate Adaptation . . 25

3.3.2 Optimal Rate Adaptation with Constant Transmit Power 27

3.3.3 Channel Inversion with Fixed Rate 28

3.4 Numerical Results and Comparisons 28
3.5 Summary 31

4 Performance Analysis of Adaptive M-QAM for Rayleigh Fading Cooperative Systems **34**
4.1 Introduction 34
4.2 Channel and System Model 35
4.3 Adaptive M-QAM Modulation 36
4.3.1 Adaptive Scheme 36
4.3.2 Outage Probability 37
4.3.3 Achievable Spectral Efficiency 39
4.3.4 Average Bit Error Rate 40
4.4 Numerical Results and Comparisons 42
4.5 Summary 44

5 Optimum Switching Adaptive M-QAM for Rayleigh Fading Cooperative Communication **48**
5.1 Introduction 48
5.2 Channel and System Model 49
5.3 Adaptive M-QAM 50
5.3.1 Five-Mode Adaptive M-QAM 50
5.3.2 Outage Probability 50
5.3.3 Achievable Spectral Efficiency 51
5.3.4 Average Bit Error Rate 51
5.4 Switching Thresholds 53
5.4.1 Fixed Switching Thresholds 53
5.4.2 Optimum Switching Thresholds 54
5.5 Numerical Results and Comparisons 58
5.6 Summary 64

6 Conclusions and Future Work **66**

6.1 Conclusions 66

6.2 Future Work 67

A Derivation for $P_{n,QAM}$ **69**

A.1 The Case of I.I.D. Fading Channels 69

A.2 The Case of Non-I.I.D. Fading Channels 73

References **74**

List of Tables

5.1 Five-Mode Adaptive M-QAM Parameters 50
5.2 M-QAM BER Parameters 52

List of Figures

1.1 Satellite relay network. 3

2.1 Cooperative diversity wireless network. 9
2.2 Transmission using TDMA. 10
2.3 System Model for Adaptive Transmission. 14

3.1 Cooperative diversity wireless network with adaptive transmission. 21
3.2 Channel capacity comparison of adaptive schemes with i.i.d. Rayleigh fading channels. 30
3.3 Outage probability of adaptive schemes with i.i.d. Rayleigh fading channels. 31
3.4 Channel capacity versus cut-off SNR γ_0^* for $\bar{\gamma}_{s,d} = \bar{\gamma}$. 32
3.5 Channel capacity comparison of adaptive schemes with non-i.i.d. Rayleigh fading channels. 32
3.6 Outage probability of adaptive schemes with non-i.i.d. Rayleigh fading channels. 33

4.1 Cooperative diversity wireless network with adaptive transmission. 35
4.2 Constellation size relative to the received SNR (dB). 38
4.3 Outage probability of adaptive schemes with i.i.d. Rayleigh fading channels. 43

4.4 Outage probability of adaptive schemes with non-i.i.d. Rayleigh fading channels. 44
4.5 Achievable rates of adaptive schemes with i.i.d. Rayleigh fading channels. 45
4.6 Achievable rates of adaptive schemes with non-i.i.d. Rayleigh fading channels. 46
4.7 Average BER for i.i.d. Rayleigh fading channels. 46
4.8 Average BER for non-i.i.d. Rayleigh fading channels. 47

5.1 Constellation size relative to the received SNR (dB). 54
5.2 Switching level constraint relationship. 56
5.3 Switching thresholds as a function of γ_1. 57
5.4 Constraint function $Y(\bar{\gamma}; \boldsymbol{s}(\gamma_1))$ for i.i.d. Rayleigh fading with $m = 1$ relay. 59
5.5 Switching thresholds for i.i.d. Rayleigh fading with $m = 1$ relay. 59
5.6 Achievable rate for i.i.d. Rayleigh fading with $m = 1$ relay. . . 61
5.7 Outage probability for i.i.d. Rayleigh fading with $m = 1$ relay. 61
5.8 Average bit error rate for i.i.d. Rayleigh fading with $m = 1$ relay. 62
5.9 Switching thresholds for non-i.i.d. Rayleigh fading with $m = 2$ relays. 62
5.10 Achievable rate for non-i.i.d. Rayleigh fading with $m = 2$ relays. 63
5.11 Outage probability for non-i.i.d. Rayleigh fading with $m = 2$ relays. 63
5.12 Average bit error rate for non-i.i.d. Rayleigh fading with $m = 2$ relays. 64

Acronyms

Acronyms	Definition
ACR	adaptive continuous rate
ADR	adaptive discrete rate
AF	amplify-and-forward
AWGN	additive white Gaussian noise
BER	bit error rate
CDF	cumulative distribution function
CDMA	code division multiple access
CSI	channel state information
CSMA/CA	carrier sense multiple access with collision avoidance
CTS	clear-to-send
DF	decode-and-forward
ETSI	European Telecommunications Standards Institute
GSM	Global System for Mobile communications
IEEE	Institute of Electrical and Electronics Engineers
i.i.d.	independent identically distributed
MAC	medium access control
MGF	moment generating function
M-QAM	M-ary quadrature amplitude modulation
MRC	maximum ratio combining
MIMO	multiple input multiple output

non-i.i.d.	non-identical independently distributed
OFDM	orthogonal frequency division multiplexing
PDF	probability density function
PHY	physical
RTS	request-to-send
SNR	signal-to-noise ratio
TDMA	time division multiple access
WiMAX	Worldwide Interoperability for Microwave Access

Chapter 1

Introduction

1.1 Motivation

WIRELESS COMMUNICATIONS HAS EXPERIENCED impressive growth lately [14]. The primary drive for such advancements is foremost due to the consumers demand. The demand for inexpensive but effective data services, such as wireless Internet access with rich video content is pushing intensive research efforts on higher-quality higher-speed wireless services [14]. The main constraint on such services is signal fading in wireless channels. Fading can be classified as either small-scale or large-scale. That is, small-scale fading is the time variation of the channel strengths due to multipath prorogation, while large-scale effects are such as path loss via distance attenuation and shadowing by obstacles [44]. However, techniques have been developed to help combat and/or exploit the effects of fading to increase the reliability (higher-quality) or the spectral efficiency (higher-speed).

Diversity techniques in space, frequency, and time are commonly used to combat the effects of fading. Diversity is achieved by making use of the multipath channel so that multiple copies of the transmitted signal are available at the receiver. For instance, multiple transmit and receive antennas can be

used to exploit space diversity; orthogonal frequency division multiplexing (OFDM) can be used to achieve frequency diversity; and repetition coding with interleaving can be used for time diversity. The most modern approach to the aforementioned techniques is MIMO (multiple input multiple output) communications where the transmitter and receiver have multiple antennas, which has been extensively studied in [44]. However, some practical situations arise where multiple antennas can not be used. For instance, in wireless sensor networks, the sensors are usually very small, require low power, and have limited hardware complexity which makes then not suited for multiple antenna transmission [42]. Furthermore, in cellular networks mobile phones have limited battery and size, making them ill suited for multiple antennas.

More recently, cooperative diversity has emerged as a technique to exploit the benefits of multiple antenna diversity by using a collection of distributed antennas belonging to multiple single-antenna devices [26]. In cooperative communications, the source transmits information to the destination not only through a direct-link but also through the use of other nodes in the network. The destination receives a copy of the transmitted signal from the source, and copies of the transmitted signal from each of the relays, resulting in multiple copies of the transmitted signal at the destination. For instance, a satellite relay is depicted in Fig. 1.1, where the mobile receive a copy of the signal directly from the satellite and duplicate version through the relay.

The development of cooperative wireless networks can been seen in the current and emerging network architectures. For instance, the use of cooperation between nodes has been implemented in mesh type networks of the IEEE 802 standards (WiMAX, Wi-Fi, ZigBee, Bluetooth) [29, 42]. A limitation of the currently implemented cooperative protocols is the ineffective use of adaptation to the time-varying channel of the wireless network. Adaptation is known to be advantageous in increasing the performance of wireless systems [1, 2, 16], as it has been discussed for cellular systems such as GSM and CDMA, and at

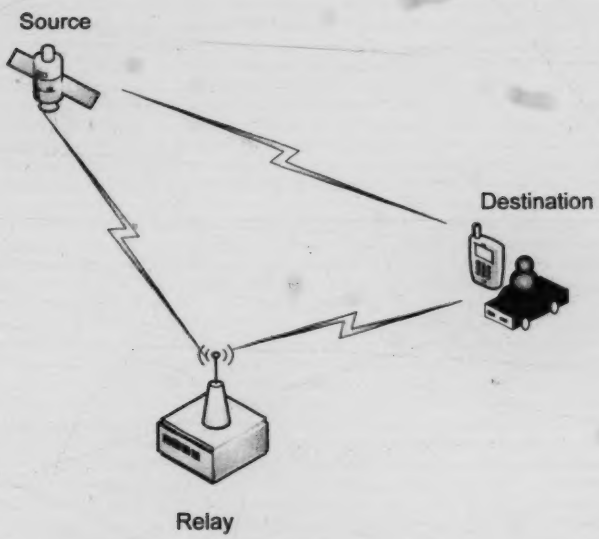

Fig. 1.1. Satellite relay network.

the physical layer of several IEEE and ETSI standards [10, 13, 33].

In adaptive transmission, the source adapts the transmit power level, symbol/bit rate, constellation size, coding rate/scheme, or any combination of these parameters in response to the changing channel conditions [1, 16]. Therefore, by transmitting faster and/or higher power under good channel conditions and slower and/or smaller power under poor conditions, a higher spectral efficiency without sacrificing performance can be achieved. Moreover, cooperative networks under adaptive transmission has not been previously analyzed and is the major contribution of this thesis.

1.2 Contributions

In this thesis, cooperative communication under adaptive transmission is analyzed. Specifically, the capacity, spectral efficiency, outage probability, and error performance are investigated under different scenarios based on practical assumptions. The contributions of this thesis can be divided into three main

parts:

- The capacity of three adaptive protocols are derived for the amplify-and-forward (AF) cooperative system over both independent and identically distributed (i.i.d.) Rayleigh fading and non-identically and independent distributed (non-i.i.d.) Rayleigh fading environments. The three different adaptive techniques considered are: (i) optimal simultaneous power and rate adaptation; (ii) constant power with optimal rate adaptation; (iii) channel inversion with fixed rate. The capacity analysis is based on an upper bound on the effective received signal-to-noise ratio (SNR). The tightness of the upper bound is validated by the use of a lower bound and by Monte Carlo simulation. The results of this contribution have been accepted to appear in an upcoming IEEE journal publication [36].

- The performance of constant-power, rate-adaptive M-ary quadrature amplitude modulation (M-QAM) transmission with an AF cooperative system is derived. Both continuous rate adaptation and discrete rate adaptation with fixed switching is considered. Expressions are derived for the outage probability, achievable spectral efficiency, and bit error rate (BER) over both i.i.d. and non-i.i.d. Rayleigh fading environments. The analysis is based on an accurate upper bound on the total effective signal-to-noise ratio SNR at the destination and is validated by Monte Carlo simulation. The results of this contribution appeared in the proceedings of the IEEE 2008 International Conference on Communication [35].

- The optimum switching levels for adaptive five-mode M-QAM transmission over an AF cooperative communication network are found. The performance analysis for adaptive five-mode M-QAM with fixed switching to meet an instantaneous BER and with optimized switching to meet an average BER are compared. Specifically, both i.i.d. and non-i.i.d.

Rayleigh fading environments are considered and the outage probability, achievable spectral efficiency, and BER are computed for both fixed switching and optimum switching. The results of this contribution have been submitted to an IEEE journal [34].

1.3 Thesis Outline

This thesis is organized as follows:

- Chapter 2 introduces the preliminary ideas of cooperative communication systems and adaptive transmission techniques. It summarizes the existing work in this area and provides the minimum background required to understand the rest of the thesis.

- Chapter 3 presents the system model for cooperative communication systems under adaptive transmission. The capacity for the AF cooperative system over both i.i.d. Rayleigh fading and non-i.i.d. Rayleigh fading environments, for three adaptive protocols is derived.

- Chapter 4 elaborates on the existing system model of Chapter 3, by applying practical adaptive M-QAM transmission. The outage probability, achievable spectral efficiency, and error rate performance for the AF cooperative system are derived. The achievable spectral efficiency of adaptive M-QAM is then compared with the theoretically capacity derived in Chapter 3.

- Chapter 5 extends the work of Chapter 4 by optimizing the switching levels for adaptive M-QAM. Specifically adaptive five-mode M-QAM is considered and the performance of the systems with optimal switching and with fixed switch (considered in Chapter 4) are compared in terms of outage probability, achievable spectral efficiency, and error rate performance.

- Chapter 6 concludes this thesis and suggests future directions.

Chapter 2

Preliminaries and Background

2.1 Cooperative Communications

MODERN WIRELESS NETWORKS consist of several users or nodes, which are potentially able to communicate with one another. These networks differ from the traditional point-to-point wireless systems, where for instance a user would strictly communicate only with a base station. Although direct communication between two nodes can be realized by point-to-point communication it is sometimes advantageous to route the transmitted information through multiple intermediate nodes. The reason behind this routing is that the wireless link between specific nodes can often be poor, and requires increased transmission power to achieve a specific reliability or quality. Furthermore, by routing the transmitted signal through several intermediate nodes an increase in power saving can occur while archiving a specific quality of service [42].

The technique of routing the transmitted signal between nodes is more formally known as cooperative communications [26, 27, 40, 41]. Recently, [26, 27, 40, 41] have investigated the achievable rate for cooperative transmission for specific protocols. Reference [26] shows that full spatial diversity can be

achieved by using cooperative communications. That is, single antenna nodes in the network can share their antennas in a manner that is similar to multiple antenna systems, to gain the well known diversity benefit of MIMO systems [44]. By relaying the transmitted information through other nodes of the network, the source ensures that the destination receives multiple independent copies of the original transmitted signal, which creates diversity.

Although there has been a resent surge in research based on the findings of [26, 27, 40, 41], the idea of information relaying has been around since the 1970's [9]. There are some differences between the original work of [9] where an information theoretical study of a single relay in additive white Gaussian noise (AWGN) is studied, and the recent surge of work with relays in wireless fading channels. For instance, the use of GSM and CDMA in [26, 27, 40, 41], the concept of diversity, performance analysis, and practical consideration are studied. It is worth mentioning that even though the information theoretical study of the relay channel has been around since the 1970's the capacity of the general relay is not even known today [12]. Furthermore, there is no specific cooperative strategy or protocol that is known to have the best performance [12], however from a practical perspective there are two cooperative protocols that are worth studying.

The two main cooperative protocols are [26]: i) amplify-and-forward (AF) and ii) decode-and-forward (DF). In the AF case the relay nodes simply amplify the received signal and re-transmit it to the destination. For the DF case the relays decode the transmitted signal, re-encode the message, not necessarily with the same codebook as the source, and transmit the re-encoded signal to the destination. Moreover, selection relaying where a subset of the relays are used to re-broadcast the signal and incremental relaying where the relay (or relays) only transmits if the direct transmission fails is presented in [26]. However, as this thesis only studies cooperative network under the AF protocol, only the specifics of AF will be presented in detail. Other protocols for

cooperative networks are described in [26].

2.1.1 Cooperative System Model

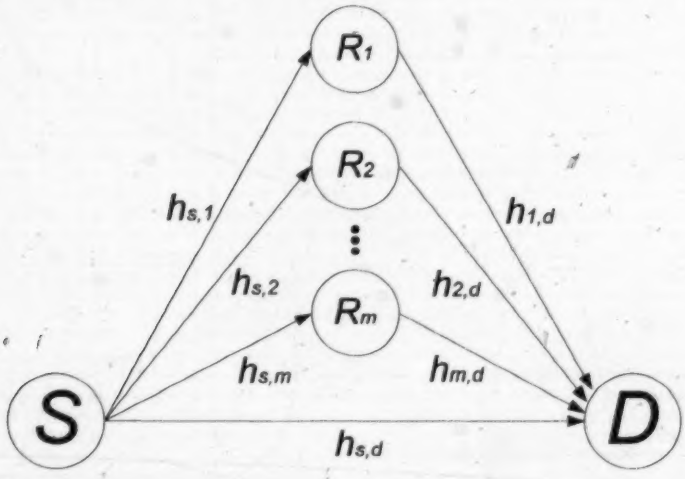

Fig. 2.1. Cooperative diversity wireless network.

Figure 2.1 presents the cooperative wireless network, where a source node S communicates with a destination node D via a direct link and through m non-regenerative or AF cooperative relays R_i, $i \in \{1, 2, ..., m\}$. In the first phase of cooperation, the source transmits the signal x to the destination and the relays. In the second phase of cooperation, the ith relay ($i = 1, 2, ..., m$) amplifies the received signal and transmits to the destination in a round robin fashion. This is illustrated in Fig. 2.2. The second phase of transmission requires m time slots to guarantee orthogonal transmission, and time division multiple access (TDMA) is required [26]. This is because of the half-duplex constraint, the practical perspective that the relays can not simultaneously transmit and receive. Furthermore, frequency division multiple access or code division multiple access could also be used so that the relays can transmit simultaneously to the destination, however at the cost of bandwidth expansion.

So without loss of generality, under the orthogonal constrain the cooperative system model can be conveniently represent using time-division notation [26].

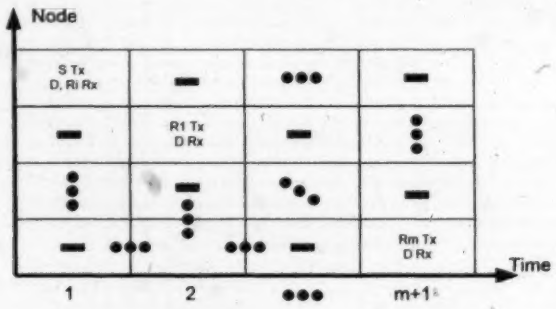

Fig. 2.2. Transmission using TDMA.

In the first phase of cooperation, the received signals at the destination and at the ith relay respectively are

$$r_{s,d} = h_{s,d}x + n_{s,d}, \tag{2.1}$$

$$r_{s,i} = h_{s,i}x + n_{s,i}, \quad i = 1, \ldots, m, \tag{2.2}$$

where $h_{s,i}$ and $h_{s,d}$ denote the Rayleigh fading coefficients between the source and the ith relay and the source and the destination, respectively. The channel coefficients are assumed i.i.d. circularly symmetric zero mean complex Gaussian random variables with unit variance, such distribution is denoted by $\mathcal{CN}(0,1)$. The noise term is denoted at the relays as $n_{s,i}$ and at the destination as $n_{s,d}$. Where the AWGN at the relays and destination is assumed to have zero mean equal variance N_0, such distribution is denoted as $\mathcal{CN}(0, N_0)$.

In the second phase of cooperation, the received signal at the destination from the ith relay is

$$r_{i,d} = G_i h_{i,d} r_{s,i} + n_{i,d}, \quad i = 1, \ldots, m, \tag{2.3}$$

where $h_{i,d}$ is the Rayleigh fading coefficient between the ith relay and destination is $\mathcal{CN}(0,1)$, the noise term $n_{i,d}$ from the ith relay at the destination

is $\mathcal{CN}(0, N_0)$ and G_i is the ith relay amplifier gain. The received ith relays signal at the destination can then be written as

$$r_{i,d} = G_i h_{i,d} \left[h_{s,i} x + n_{s,i} \right] + n_{i,d}. \tag{2.4}$$

At the destination node, using maximum ratio combining (MRC) the total SNR can easily be found to be [19, 26]

$$\begin{aligned} \gamma_{\text{tot}} &= |h_{s,d}|^2 E_s / N_0 + \sum_{i=1}^{m} \frac{E_s |h_{s,i}|^2 |h_{i,d}|^2 G_i^2}{\left[|h_{i,d}|^2 G_i^2 + 1 \right] N_0} \\ &= |h_{s,d}|^2 E_s / N_0 + \sum_{i=1}^{m} \frac{\frac{E_s |h_{s,i}|^2}{N_0} \frac{E_s |h_{i,d}|^2}{N_0}}{\frac{E_s |h_{i,d}|^2}{N_0} + \frac{E_s}{G^2 N_0}} \end{aligned} \tag{2.5}$$

where E_s is the average symbol energy, and N_0 is the noise variance. Equation (2.5) shows that the equivalent SNR is dependent on the choice of the relay gains G_i. Choosing the relay gain as in [26],

$$G_i^2 = E_s / \left(E_s |h_{s,i}|^2 + N_0 \right), \tag{2.6}$$

the resulting equivalent SNR is

$$\gamma_{\text{tot}} = \gamma_{s,d} + \sum_{i=1}^{m} \frac{\gamma_{s,i} \gamma_{i,d}}{\gamma_{s,i} + \gamma_{i,d} + 1}, \tag{2.7}$$

where $\gamma_{s,i} = |h_{s,i}|^2 E_s / N_0$ is the instantaneous SNR between S and R_i, $\gamma_{i,d} = |h_{i,d}|^2 E_s / N_0$ is the instantaneous SNR between R_i and D, $\gamma_{s,d} = |h_{s,d}|^2 E_s / N_0$ is the instantaneous SNR between S and D. The choice of the gain G_i is such that it limits the output power of the relay when the fading between the source and the ith relay is low [19].

Now that the system model for the cooperative communication system is defined, the performance analysis of the model can be conducted. As the total effective SNR can be formulated, the standard analysis considered in traditional communication systems can easily be extended to cooperative communication systems. The cooperative system model presented above will be used through this thesis.

It is also worth mentioning that in wireless networks there is the problem that two transmitting nodes cannot sense each other and will often interfere with each other. This problem is often combated using carrier sense multiple access with collision avoidance (CSMA/CA) control frames [39]. How CSMA/CA control frames work is that they are used to reserve the transmission channel for a data packet before the packet is transmitted. That is, the sender transmits a request-to-send (RTS) frame to the receiver and after receiving, the receiver sends out a clear-to-send (CTS) frame to respond to the sender. The neighboring nodes after receiving the RTS and CTS frames check the duration field and halts transmission for that time duration. For networks where CSMA/CA protocol is used in the medium access control (MAC) layer, the use of symbol level relaying at the physical (PHY) layer is suitable as long as the RTS and CTS are limited in the number of symbols. As the relay process requires the addition of m time slots per a symbol, it is important that the RTS and CTS are limited so that they do not substantially interfere with neighboring nodes. Although the research considered in this thesis is conducted at the symbol level it is assumed that MAC layer control can easily be applied.

2.2 Adaptive Transmission

Signal fading is a fundamental challenge in wireless communications. That is, rapid variations of channel gain due to multipath prorogation can dramatically reduce the reliability. However, adaptive wireless transmission techniques are known to cope with the time varying nature of the wireless channel, by changing the transmission parameters according to the channel quality. The limited availability of wireless spectrum is another challenge. This lack of available spectrum for expansion of wireless services required more spectrally efficient communication in order to meet the consumer demand. As this is the case,

adaptive transmission techniques are considered a top candidate to increase the spectral efficiency in many wireless systems and standards [10, 13, 33].

Adaptive transmission works by the receiver estimating the channel and feeding back the channel state information (CSI) to the transmitter. The transmitter then adapts the transmit power level, symbol/bit rate, constellation size, coding rate/scheme or any combination of these parameters in response to the changing channel conditions [1, 16]. The source may transmit faster and/or at a higher power under good channel conditions and slower and/or at a reduced power under poor conditions. As classical wireless communication systems are generally designed with the worst case channel in mind, to maintain a fixed quality of service, adaptation allows for a higher spectral efficiency without sacrificing performance.

Recently there has been a surge of research in the area of adaptive transmission techniques for traditional point-to-point communication systems as can be seen in [2, 15, 16, 38, 45, 46], and the extension to systems with different diversity techniques in [1, 8, 25, 31, 49]. This surge of research is primarily due to the work of [16] where the Shannon capacity of a fading channel under several adaptive policies is obtained. However, it is worth noting that adaptive techniques have been around since the 1960's [7, 20], but have not been practical till recent advancements in computing technologies. The techniques of variable power adaptation and/or variable rate adaptation are applicable in many practical wireless communication systems and specifically there are three protocols worth studying.

The three adaptive protocols are [1, 2, 16]: (i) optimal simultaneous power and rate adaptation, (ii) constant power with optimal rate adaptation, (iii) channel inversion with fixed rate. The first protocol optimal simultaneous power and rate adaptation, varies its power level and rate parameters in response to the changing channel conditions. The second protocol is similar to the first, and differs by fixing its transmit power level and adapts only its data

rate. The third protocol is quite different then the first two protocols as it maintains constant rate and adapts its power to the inverse of the channels fading. More specifically, the first protocol achieves the ergodic capacity of the system; that is, the maximum average rate achievable by use of adaptive transmission [16, 31]. The problem with simultaneous power and rate adaptation is that some applications require fixed rate, making this technique not suitable for all applications. In the second protocol, the transmitter adapts its rate only while maintaining a fixed power level. Thus, this protocol can be implemented at reduced complexity and is more practical than that of optimal simultaneous power and rate adaptation. The third protocol achieves what is known as the outage capacity of the system; that is the maximum constant data rate the can be supported for all channel conditions with some probability of outage [31]. However, the capacity of channel inversion is always less than the capacity of the previous two protocols as the transmission rate is fixed. On the other hand, constant rate transmission is required in some applications and is worth the loss in achievable capacity.

2.2.1 Adaptive Transmission System Model

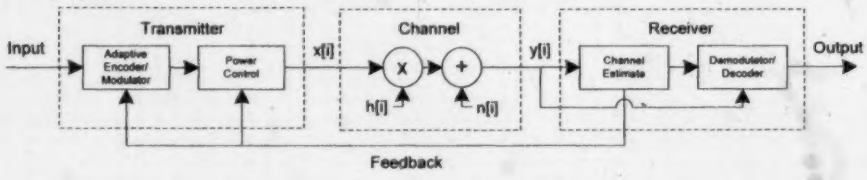

Fig. 2.3. System Model for Adaptive Transmission.

In Fig. 2.3, the system model for an adaptive transmission wireless communication system is illustrated, based on the model in [14]. The transmitter firstly applies some form of adaptive coding and/or modulation, followed by power control. The power level, modulation format, encoder structure is

adapted based on the feedback of the received SNR. Based on this feedback the symbol $x[i]$ at time i, is transmitted. A wireless channel with gain $h[i]$ and AWGN noise $n[i]$ is applied, the received symbol is denoted as $y[i]$. The receiver then estimates the channel $\widehat{h}[i]$ decodes and demodulates accordingly, and feedbacks the channel estimate. How frequent the channel gain $h[i]$ varies will effectively determine how often the transmitter will adjust its transmission parameters of the encoder/modulator and power controller. For this system model to be valid the channel must be slow fading, that is the channel gain remains constant over multiple symbol durations. The reasons for this is the channel estimator must be able to make a very accurate estimate and so the delay of the feedback path is effectively negligible. As this assumption is valid for many practical situations, the following assumption is made, for the remaining analysis in this thesis, that error-free channel estimation occurs and that error-free delay-free feedback of the channel estimate from the receiver to the transmitter occurs.

It is well-known that the Shannon capacity of the fading channel defines the theoretical upper bound on the rate for reliable data transmission. That is, the capacity can be used as a metric in which to compare the throughput of practical communication systems to. The capacity for adaptive transmission for the three aforementioned protocols has been shown in [16] and is as follow.

Optimal Simultaneous Power and Rate Adaptation

The channel capacity C_{opra} (in bits/second) given the probability density function (PDF) of the received SNR $p_\gamma(\gamma)$, under the condition of optimal simultaneous power and rate adaptation is given by [1, 16]:

$$C_{\text{opra}} = \frac{B}{\ln 2} \int_{\gamma_0}^{\infty} \ln\left(\frac{\gamma}{\gamma_0}\right) p_\gamma(\gamma) d\gamma, \tag{2.8}$$

where B (in hertz) is the bandwidth of the channel and γ_0 is the optimal cutoff SNR below which the transmission is stopped.

The optimal cutoff SNR below which the transmission is halted satisfies

$$\int_{\gamma_0}^{\infty} \left(\frac{1}{\gamma_0} - \frac{1}{\gamma}\right) p_\gamma(\gamma) d\gamma = 1. \tag{2.9}$$

As the transmission is halted when $\gamma < \gamma_0$, there is a probability that the SNR falls below the optimal threshold γ_0. This outage probability is given by:

$$P_{\text{out}} = P[\gamma < \gamma_0] = \int_0^{\gamma_0} p_\gamma(\gamma) d\gamma = 1 - \int_{\gamma_0}^{\infty} p_\gamma(\gamma) d\gamma. \tag{2.10}$$

Optimal Rate Adaptation with Constant Transmit Power

For optimal rate adaptation with constant transmit power, the channel capacity C_{ora} is given by [1, 16]:

$$C_{\text{ora}} = \frac{B}{\ln 2} \int_0^{\infty} \ln(1+\gamma) p_\gamma(\gamma) d\gamma. \tag{2.11}$$

Channel Inversion with Fixed Rate

Truncated channel inversion is possible as long as the received SNR is above a cutoff γ_0. The channel capacity C_{tifr} is given by [1, 16]:

$$C_{\text{tifr}} = \frac{B}{\ln 2} \ln\left(1 + \left[\int_{\gamma_0}^{\infty} \frac{p_\gamma(\gamma) d\gamma}{\gamma}\right]^{-1}\right)(1 - P_{\text{out}}). \tag{2.12}$$

Now that the system model for the wireless communication system under adaptive transmission is defined and the capacity under different protocols is defined, the capacity of any system model can be derived as long as the received SNR can be statistically formulated. This is because, all of the three capacity equations defined have a common metric of the PDF of the received SNR. As the capacity of a communication channel defines the upper bound on the amount of information that can be reliably transmitted, the capacity of adaptive transmission was only presented in this section as it can be used as a benchmark for practical systems to achieve. For a more elaborate discussion on adaptive transmission techniques, applications and performance analysis see [14, Ch. 9].

2.3 Summary

The system models for cooperative communication and adaptive transmission are defined. The AF cooperative network receive SNR was formulated. Furthermore, the capacity expressions of adaptive transmission has been mentioned. If the PDF of the receive SNR for the cooperative network can be derived then the capacity of the cooperative network under adaptive transmission can be found. The analysis of the capacity of the cooperative network under adaptive transmission will be the concern of the next chapter, followed by chapters on practical techniques to achieve this capacity.

Chapter 3

Channel Capacity of Cooperative Communication Under Adaptive Transmission

3.1 Introduction

AN EFFICIENT WAY OF PROVIDING DIVERSITY in wireless fading networks is through the use of node cooperation for information relaying [26, 40][1]. In cooperative communications, the source transmits information to the destination not only through a direct-link but also through the use of relays. This so-called "cooperative diversity" can dramatically improve the performance by using the antennas available at the other nodes of the network.

The performance of cooperative communication systems has been analyzed for various system and channel models. The average symbol error rate (SER) of a two-hop cooperative system is analyzed in [3, 19, 23] for the Rayleigh and Nakagami-m fading channels. The outage performance of the cooperative sys-

[1] *A version of this chapter has been accepted for publication in IEEE Transactions on Wireless Communications.*

tem with Rayleigh fading which operates on a half-duplex mode in the low SNR regime is provided in [4]. In [5] and [43] the authors derive closed-form expressions for the outage probability for Rayleigh and Nakagami-m channels, respectively, with decode-and-forward relays. The performance of an analytical model for automatic repeat request (ARQ) cooperative diversity in multihop wireless networks is presented in [28]. Furthermore, the enhancement of spatial-diversity by applying space-time coding is investigated in [6] and [47] for non-regenerative and distributed regenerative relaying, respectively.

All the aforementioned papers only consider fixed rate and fixed power transmission. However, adaptive transmission techniques for the wireless channel are shown to be effective [1, 16]. Particularly, the transmitter adapts the transmit power level, symbol/bit rate, constellation size, coding rate/scheme or any combination of these parameters in response to the changing channel conditions [1,16]. Therefore, by transmitting faster and/or higher power under good channel conditions and slower and/or smaller power under poor channel conditions, a higher spectral efficiency without sacrificing performance can be achieved.

More recently, resource allocation in terms of power and bandwidth is investigated for the basic three-node relay network in [18,21,24,30] and for the m-node relay network in [32,37,48]. The majority of the aforementioned work considers power allocation problems in the context of cooperative networks. This problem is formulated by placing a fixed power constraint among the relays, and one seeks to allocate the power to different nodes to optimize some objective. This requires channels state information (CSI) of all the links and fixed source rates, and as a consequence, it is distinctly different than the adaptive policies of [1, 16]. In general, the power allocation problem has a high overhead when the number of nodes in the network is large. This is due to the requirement of having the CSI for all of the links. Furthermore, rate adaptation at the transmitter is not considered in all the aforementioned work.

Motivated by these observations, this chapter propose the use of fixed non-regenerative cooperative systems with adaptive transmission techniques. That is, only the source adapts its rate and/or power level according to the changing channel conditions, while the m relays simply amplify and forward the signals. For the proposed source-adaptation scheme only partial CSI is required at the source. Thus, feedback of the effective SNR is only required to be available at the source, not the m relays. In this chapter, the upper bound expressions for the capacity and outage probability of such source-adaptive cooperative networks in both i.i.d. and non-i.i.d. Rayleigh fading environments are derived. A lower bound and Monte Carlo simulations are used to substantiate the tightness of the derived upper bound. Three different adaptive techniques are considered, namely (i) optimal simultaneous power and rate adaptation, (ii) constant power with optimal rate adaptation, (iii) channel inversion with fixed rate.

The remainder of this chapter is organized as follows. Section 3.2 presents the channel and system model. The capacity analysis for the cooperative system under the different adaptive transmission techniques is derived in Section 3.3. In Section 3.4 the results of the capacity derivations are compared. A summary is given in Section 3.5.

3.2 Channel and System Model

3.2.1 System Model

The adaptive cooperative wireless network of Fig. 3.1, a source node S communicates with a destination node D via a direct link and through m AF relays R_i, $i \in \{1, 2, ..., m\}$. This model is similar to the model discussed in Chapter 2, and the important points of the model will be briefly reviewed. In the first phase of cooperation, the source transmits the signal x to the desti-

nation and the relays. The received signals at the destination and at the ith relay respectively are

$$r_{s,d} = h_{s,d}x + n_{s,d}, \tag{3.1}$$

$$r_{s,i} = h_{s,i}x + n_{s,i}, \quad i = 1, \ldots, m, \tag{3.2}$$

where $h_{s,i}$, $h_{i,d}$, and $h_{s,d}$ denote the Rayleigh fading coefficients between the source and the ith relay, the ith relay and destination, and the source and the destination, respectively. The noise is denoted at the relays as $n_{s,i}$ and at the destination as $n_{s,d}$ and $n_{i,d}$.

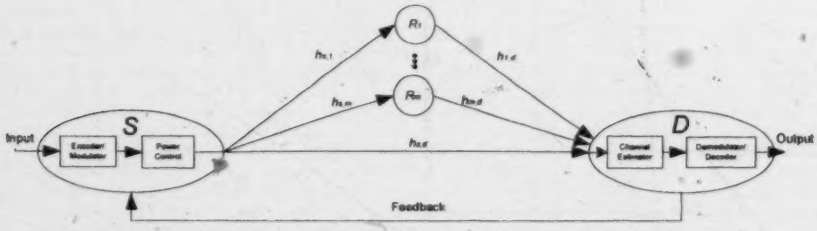

Fig. 3.1. Cooperative diversity wireless network with adaptive transmission.

The ith relay amplifies the received signal and transmits it to the destination in the second phase of cooperation. During this phase, orthogonal transmission is required to transmit the m symbols at each of the relays. Without lost of generality, this can be accomplished by using TDMA [26]. That is, each of the m symbols are transmitted from the relays in a round robin fashion. The received signal at the destination from the ith relay is

$$r_{i,d} = G_i h_{i,d} r_{s,i} + n_{i,d}, \quad i = 1, \ldots, m, \tag{3.3}$$

where G_i is the ith relay amplifier gain, chosen as [26], $G_i^2 = E_s/\left(E_s|h_{s,i}|^2 + N_0\right)$ where E_s is the average symbol energy, and N_0 is the noise variance.

Using MRC at the destination node the total SNR is easily found as [26]

$$\gamma_{\text{tot}} = \gamma_{s,d} + \sum_{i=1}^{m} \frac{\gamma_{s,i}\gamma_{i,d}}{\gamma_{s,i} + \gamma_{i,d} + 1}, \tag{3.4}$$

where $\gamma_{s,i} = |h_{s,i}|^2 E_s/N_0$, $\gamma_{i,d} = |h_{i,d}|^2 E_s/N_0$, $\gamma_{s,d} = |h_{s,d}|^2 E_s/N_0$ are the instantaneous SNRs between S and R_i, R_i and D, S and D respectively.

An upper bound of the total SNR at the destination node can be found as [3, 23]

$$\gamma_{\text{tot}} \leq \gamma_{s,d} + \sum_{i=1}^{m} \gamma_i = \gamma_{ub}, \tag{3.5}$$

where $\gamma_i = \min(\gamma_{s,i}, \gamma_{i,d})$. The subsequent analysis exclusive relies on the upper bound, γ_{ub}. Furthermore, this upper bound has been shown to be quite accurate [3, 23]. A lower bound can be formulated as in [3] where $\gamma_i = 0.5 \min(\gamma_{s,i}, \gamma_{i,d})$. As the lower bound is different from the upper bound only by a factor of half, the following analysis can easily be extended to the lower bound, but is omitted for brevity.

3.2.2 Probability Distribution Function Derivation

As γ_i and $\gamma_{s,d}$ are independent, the moment generating function (MGF) of γ_{ub} is expressed as

$$M_{\gamma_{ub}}(s) = M_{\gamma_{s,d}}(s) \prod_{i=1}^{m} M_{\gamma_i}(s), \tag{3.6}$$

where $M_{\gamma_{s,d}}(s)$ and $M_{\gamma_i}(s)$ are the MGF of $\gamma_{s,d}$ and γ_i, respectively, and the MGF is defined as $M_X(s) = \mathbf{E}\{e^{-sX}\}$, $\mathbf{E}\{\cdot\}$ denotes the statistical average over the random variable X.

For Rayleigh fading, $\gamma_{s,d}$ is exponentially distributed, thus $M_{\gamma_{s,d}}(s) = (1 + \bar{\gamma}_{s,d}s)^{-1}$, where $\bar{\gamma}_{s,d} = \mathbf{E}\{|h_{s,d}|^2\} E_s/N_0$. The MGF of γ_i is derived via the use of the cumulative distribution function (CDF) of γ_i

$$F_{\gamma_i}(\gamma) = 1 - P(\gamma_{s,i} > \gamma) P(\gamma_{i,d} > \gamma). \tag{3.7}$$

To proceed further, consider two different cases of fading channels as follows.

I.I.D. Fading Channels

In this case, the statistic of all links is identical and the average SNR on each link is given by $\bar{\gamma} = \mathbf{E}\{|h_{s,i}|^2\}E_s/N_0 = \mathbf{E}\{|h_{i,d}|^2\}E_s/N_0$. Differentiating (3.7) the PDF of γ_i is easily shown to be $p_{\gamma_i}(\gamma) = (2/\bar{\gamma})e^{-2\gamma/\bar{\gamma}}$. Then, the MGF can be written as $M_{\gamma_i}(s) = (1 + 0.5\bar{\gamma}s)^{-1}$. Applying these results into (3.6) the expression for the MGF of γ_{ub} is

$$M_{\gamma_{ub}}(s) = (1 + \bar{\gamma}_{s,d}s)^{-1}(1 + 0.5\bar{\gamma}s)^{-m}. \tag{3.8}$$

Using partial fractions, (3.8) can be rewritten as

$$M_{\gamma_{ub}}(s) = \beta_0(1 + \bar{\gamma}_{s,d}s)^{-1} + \sum_{i=1}^{m} \beta_i(1 + 0.5\bar{\gamma}s)^{-i}, \tag{3.9}$$

where

$$\beta_0 = \left(1 - \frac{\bar{\gamma}}{2\bar{\gamma}_{s,d}}\right)^{-m} \text{ and } \beta_i = \frac{(0.5\bar{\gamma})^{(i-m)}}{(m-i)!}\frac{\partial^{m-i}}{\partial s^{m-i}}\left[(1 + \bar{\gamma}_{s,d}s)^{-1}\right]_{s=-1/(0.5\bar{\gamma})}. \tag{3.10}$$

Taking the inverse Laplace transform of $M_{\gamma_{ub}}(s)$ in (3.9), and using the fact that $\mathcal{L}^{-1}\{(1 + as)^{-k}\} = \frac{1}{(k-1)!a^k}x^{k-1}e^{-\frac{x}{a}}$, the pdf of γ_{ub} is as follows:

$$p_{\gamma_{ub}}(\gamma) = \frac{\beta_0}{\bar{\gamma}_{s,d}}e^{-\frac{\gamma}{\bar{\gamma}_{s,d}}} + \sum_{i=1}^{m} \frac{\beta_i(0.5\bar{\gamma})^{-i}}{(i-1)!}\gamma^{i-1}e^{-\frac{\gamma}{(0.5\bar{\gamma})}}. \tag{3.11}$$

Non-I.I.D. Fading Channels

In practice, the relays are often not symmetrically placed which causes different fading statistics among the relay-destination links. Thus, it is of interest to consider independent but not identically distributed channels. Similar to the case of i.i.d. fading, differentiating (3.7) we obtain the pdf of γ_i as $p_{\gamma_i}(\gamma) = (1/\tau_i)e^{-\gamma/\tau_i}$, where $\tau_i = \frac{\bar{\gamma}_{s,i}\bar{\gamma}_{i,d}}{\bar{\gamma}_{s,i}+\bar{\gamma}_{i,d}}$, $\bar{\gamma}_{s,i} = \mathbf{E}\{|h_{s,i}|^2\}E_s/N_0$ and $\bar{\gamma}_{i,d} = \mathbf{E}\{|h_{i,d}|^2\}E_s/N_0$. The MGF can then be written as $M_{\gamma_i}(s) = (1+\tau_i s)^{-1}$. Applying these results into (3.6) the MGF of γ_{ub} is

$$M_{\gamma_{ub}}(s) = (1 + \bar{\gamma}_{s,d}s)^{-1}\prod_{i=1}^{m}(1 + \tau_i s)^{-1}. \tag{3.12}$$

Again, using partial fractions, (3.12) can be rewritten

$$M_{\gamma_{ub}}(s) = \widehat{\beta}_0(1+\gamma_{s,d}s)^{-1} + \sum_{i=1}^{m} \widehat{\beta}_i(1+\tau_i s)^{-1}, \tag{3.13}$$

where

$$\widehat{\beta}_0 = \prod_{i=1}^{m}\left(1-\frac{\tau_i}{\bar{\gamma}_{s,d}}\right)^{-1} \text{ and } \widehat{\beta}_i = \left(1-\frac{\bar{\gamma}_{s,d}}{\tau_i}\right)^{-1}\prod_{k=1.k\neq i}^{m}\left(1-\frac{\tau_k}{\tau_i}\right)^{-1}, \quad i=1,\ldots,m. \tag{3.14}$$

Taking the inverse Laplace transform of $M_{\gamma_{ub}}(s)$ in (3.13) gives the pdf of γ_{ub} as:

$$p_{\gamma_{ub}}(\gamma) = \frac{\widehat{\beta}_0}{\bar{\gamma}_{s,d}}e^{-\frac{\gamma}{\bar{\gamma}_{s,d}}} + \sum_{i=1}^{m}\frac{\widehat{\beta}_i}{\tau_i}e^{-\frac{\gamma}{\tau_i}}. \tag{3.15}$$

The next section investigates the capacity of the cooperative system under adaptive transmission. In the proposed system, only the source performs adaptation, i.e., the source will vary its rate and/or power while the relays simply amplify and forward their received signal. In order to implement adaptive transmission, it is assumed that the received SNR γ_{tot} is perfectly tracked at the destination and is then fed back error free to the source. The channel is assumed to be slow fading and feedback delay is negligible, thus allowing the source to change the power and/or rate. These are more or less standard assumptions in [1, 2, 15, 16, 31].

3.3 Capacity Analysis Under Adaptive Transmission

It is well-known that the Shannon capacity of the fading channel defines the theoretical upper bound on the rate for reliable data transmission. One way to achieve this bound is to employ adaptive transmission, i.e., the transmitter at the source adapts its power, rate, and/or coding scheme to the channel variation. For fixed AF relaying where only the source performs adaptation, the capacity of different adaptive schemes are as follows.

3.3.1 Optimal Simultaneous Power and Rate Adaptation

I.I.D. Fading Channels

The channel capacity C_{opra} (in bits/second) given the pdf of the received SNR $p_{\gamma_{ub}}(\gamma)$, under the condition of optimal simultaneous power and rate adaptation is given by [1, 16]:

$$C_{\text{opra}} = \frac{B}{(m+1)\ln 2}\int_{\gamma_0}^{\infty} \ln\left(\frac{\gamma}{\gamma_0}\right) p_{\gamma_{ub}}(\gamma)d\gamma, \tag{3.16}$$

where B (in hertz) is the bandwidth of the channel and γ_0 is the optimal cutoff SNR below which the transmission is stopped. The factor $1/(m+1)$ accounts for the fact that the transmission process takes place in $(m+1)$ orthogonal channels or time-slots.

The optimal cutoff SNR below which the transmission is halted satisfies

$$\int_{\gamma_0}^{\infty}\left(\frac{1}{\gamma_0}-\frac{1}{\gamma}\right)p_{\gamma_{ub}}(\gamma)d\gamma = 1. \tag{3.17}$$

As the transmission is halted when $\gamma_{ub} < \gamma_0$, there is a probability that the SNR falls below the optimal threshold γ_0. This outage probability is given by:

$$P_{\text{out}} = P[\gamma_{ub} < \gamma_0] = \int_0^{\gamma_0} p_{\gamma_{ub}}(\gamma)d\gamma = 1 - \int_{\gamma_0}^{\infty} p_{\gamma_{ub}}(\gamma)d\gamma. \tag{3.18}$$

The capacity C_{opra} is achieved when the source adapts its power and rate simultaneously according to the perfect CSI at the transmitter. Substituting (3.11) into (3.16), and making use of the integral $\mathcal{J}_n(\mu) = \int_1^{\infty} t^{n-1}\ln(t)e^{-\mu t}dt$, $\mu > 0$; $n = 1, 2, \ldots$, which is evaluated in closed-form [1, eq. (70)], the closed-form expression for C_{opra} is

$$C_{\text{opra}} = \frac{B}{(m+1)\ln 2}\left[\frac{\beta_0\gamma_0}{\bar{\gamma}_{s,d}}\mathcal{J}_1\left(\frac{\gamma_0}{\bar{\gamma}_{s,d}}\right) + \sum_{i=1}^{m}\frac{\beta_i(0.5\bar{\gamma})^{-i}}{(i-1)!\gamma_0^{-i}}\mathcal{J}_i\left(\frac{2\gamma_0}{\bar{\gamma}}\right)\right]. \tag{3.19}$$

The optimal cutoff SNR γ_0 is found by solving for γ_0 in (3.17), which can be rewritten as

$$\frac{1}{\gamma_0}\int_{\gamma_0}^{\infty} p_{\gamma_{ub}}(\gamma)d\gamma - \int_{\gamma_0}^{\infty}\frac{1}{\gamma}p_{\gamma_{ub}}(\gamma)d\gamma = 1. \tag{3.20}$$

First,

$$\int_{\gamma_0}^{\infty} p_{\gamma_{ub}}(\gamma)d\gamma = \beta_0 e^{-\frac{\gamma_0}{\bar{\gamma}_{s,d}}} + e^{-\frac{2\gamma_0}{\bar{\gamma}}} \sum_{i=1}^{m} \beta_i \sum_{k=0}^{i-1} \frac{1}{k!} \left(\frac{2\gamma_0}{\bar{\gamma}}\right)^k \tag{3.21}$$

is established by using [17, eq. (3.351.2)]. Second,

$$\int_{\gamma_0}^{\infty} \frac{p_{\gamma_{ub}}(\gamma)d\gamma}{\gamma} = \frac{\beta_0}{\bar{\gamma}_{s,d}} E_1\left(\frac{\gamma_0}{\bar{\gamma}_{s,d}}\right) + \frac{2\beta_1}{\bar{\gamma}} E_1\left(\frac{2\gamma_0}{\bar{\gamma}}\right) + e^{-\frac{2\gamma_0}{\bar{\gamma}}} \sum_{i=2}^{m} \frac{\beta_i}{(i-1)} \sum_{k=0}^{i-2} \frac{\gamma_0^k}{k!(0.5\bar{\gamma})^{k+1}} \tag{3.22}$$

is found similarly using [17, eq. (3.351.2)] where $E_n(x)$ is the exponential integral of order n, defined by [1] $E_n(x) = \int_1^{\infty} t^{-n} e^{-xt} dt$, $x \geq 0$. Substituting (3.21) and (3.22) into (3.20) the optimal cutoff SNR γ_0 can be obtained numerically. Asymptotically as $\bar{\gamma} = \bar{\gamma}_{s,d} \to \infty$, $\gamma_0 \to 1$. Numerical results also indicate, but not shown, that γ_0 lies in the interval of $[0, 1]$.

The probability of outage is found by substituting (3.21) into (3.18)

$$P_{\text{out}} = 1 - \left[\beta_0 e^{-\frac{\gamma_0}{\bar{\gamma}_{s,d}}} + e^{-\frac{2\gamma_0}{\bar{\gamma}}} \sum_{i=1}^{m} \beta_i \sum_{k=0}^{i-1} \frac{1}{k!} \left(\frac{2\gamma_0}{\bar{\gamma}}\right)^k\right]. \tag{3.23}$$

Non-I.I.D. Fading Channels

The closed-form expression for C_{opra} is

$$C_{\text{opra}} = \frac{B}{(m+1)\ln 2} \left[\frac{\widehat{\beta}_0 \gamma_0}{\bar{\gamma}_{s,d}} \mathcal{J}_1\left(\frac{\gamma_0}{\bar{\gamma}_{s,d}}\right) + \sum_{i=1}^{m} \frac{\widehat{\beta}_i \gamma_0}{\tau_i} \mathcal{J}_1\left(\frac{\gamma_0}{\tau_i}\right)\right]. \tag{3.24}$$

The optimal cutoff SNR γ_0 in (3.24) is found by numerically solving for γ_0 in (3.20), where

$$\int_{\gamma_0}^{\infty} p_{\gamma_{ub}}(\gamma)d\gamma = \widehat{\beta}_0 e^{-\frac{\gamma_0}{\bar{\gamma}_{s,d}}} + \sum_{i=1}^{m} \widehat{\beta}_i e^{-\frac{\gamma_0}{\tau_i}}, \tag{3.25}$$

and,

$$\int_{\gamma_0}^{\infty} \frac{p_{\gamma_{ub}}(\gamma)d\gamma}{\gamma} = \frac{\widehat{\beta}_0}{\bar{\gamma}_{s,d}} E_1\left(\frac{\gamma_0}{\bar{\gamma}_{s,d}}\right) + \sum_{i=1}^{m} \frac{\widehat{\beta}_i}{\tau_i} E_1\left(\frac{\gamma_0}{\tau_i}\right). \tag{3.26}$$

As in the case of i.i.d. fading, the probability of outage is found by substituting (3.25) into (3.18)

$$P_{\text{out}} = 1 - \left[\widehat{\beta}_0 e^{-\frac{\gamma_0}{\bar{\gamma}_{s,d}}} + \sum_{i=1}^{m} \widehat{\beta}_i e^{-\frac{\gamma_0}{\tau_i}}\right]. \tag{3.27}$$

3.3.2 Optimal Rate Adaptation with Constant Transmit Power

I.I.D. Fading Channels

For optimal rate adaptation with constant transmit power, the channel capacity C_{ora} is given by [1, 16]:

$$C_{\text{ora}} = \frac{B}{(m+1)\ln 2}\int_0^\infty \ln(1+\gamma)p_{\gamma_{\text{sub}}}(\gamma)d\gamma. \tag{3.28}$$

Substituting (3.11) into (3.28), and making use of the integral $\mathcal{I}_n(\mu) = \int_0^\infty t^{n-1}\ln(1+t)e^{-\mu t}dt,\ \mu > 0;\ n = 1, 2, ...,$ which can be evaluated in a closed-form as in [1, eq. (78)], the closed-form expression for the capacity C_{ora} is

$$C_{\text{ora}} = \frac{B}{(m+1)\ln 2}\left[\frac{\beta_0}{\bar{\gamma}_{s,d}}\mathcal{I}_1\left(\frac{1}{\bar{\gamma}_{s,d}}\right) + \sum_{i=1}^{m}\frac{\beta_i(0.5\bar{\gamma})^{-i}}{(i-1)!}\mathcal{I}_i\left(\frac{2}{\bar{\gamma}}\right)\right]. \tag{3.29}$$

Non-I.I.D. Fading Channels

Likewise, the closed-form expression for the capacity C_{ora} is

$$C_{\text{ora}} = \frac{B}{(m+1)\ln 2}\left[\frac{\widehat{\beta}_0}{\bar{\gamma}_{s,d}}\mathcal{I}_1\left(\frac{1}{\bar{\gamma}_{s,d}}\right) + \sum_{i=1}^{m}\frac{\widehat{\beta}_i}{\tau_i}\mathcal{I}_1\left(\frac{1}{\tau_i}\right)\right]. \tag{3.30}$$

As the transmitter only adapts its rate, instead of both rate and power, to the changing channel conditions, the scheme of optimal rate adaptation with constant transmit power can be implemented at reduced complexity, and thus, is more practical than that of optimal simultaneous power and rate adaptation. Furthermore, as discussed in [1], (3.28) is the capacity of a flat-fading $(m+1)$ orthogonal wireless channel, without adaptation. Therefore, optimal rate adaptation with constant power is a practical technique to achieve the flat-fading channel capacity.

3.3.3 Channel Inversion with Fixed Rate

I.I.D. Fading Channels

Truncated channel inversion with fixed rate is the least complex adaptive technique as the transmitter only adjusts the power level to provide a constant SNR at the destination. Truncated channel inversion is possible as long as the received SNR is above a cutoff γ_0. This scheme achieves the outage capacity of the system. The channel capacity C_{tifr} is given by [1, 16]:

$$C_{\text{tifr}} = \frac{B}{(m+1)\ln 2} \ln\left(1 + \left[\int_{\gamma_0}^{\infty} \frac{p_{\gamma_{sb}}(\gamma)d\gamma}{\gamma}\right]^{-1}\right)(1 - P_{\text{out}}). \tag{3.31}$$

The truncated channel inversion capacity with fixed rate is simply found by substituting (3.22) and (3.23) into (3.31) but omitted here for brevity.

Non-I.I.D. Fading Channels

The truncated channel inversion capacity with fixed rate is similarly found by substituting (3.26) and (3.27) into (3.31) but is omitted for brevity.

The capacity of this scheme is shown to be always less then the previous two schemes as it does not perform rate adaptation relative to the channel conditions. It should be noted that when channel inversion is done without truncation i.e., $\gamma_0 = 0$, the capacity is zero for i.i.d Rayleigh fading. However, some applications require constant rate even with the loss in achievable capacity.

3.4 Numerical Results and Comparisons

This section presents, the channel capacity and the outage probability for cooperative systems with adaptive transmissions. For i.i.d. and non-i.i.d Rayleigh fading, the system with one relay, $m = 1$ and two relays, $m = 2$ is considered, respectively. However, the results of Section 3.3 can be used for any number

of relays. Moreover, the average SNR of the links are chosen to represent a practical model of a cooperative communication system.

In Fig. 3.2 a closed-form channel capacity derived in (3.19), (3.29), and (3.31) are plotted for i.i.d. Rayleigh fading, with $\bar{\gamma}_{s,d} = \bar{\gamma}$. Note that the approximate lower bound of [3] where $\gamma_i = 0.5 \min(\gamma_{s,i}, \gamma_{i,d})$ is also plotted along with the Monte Carlo simulation results for the case of simultaneous power and rate adaptation where 5×10^3 samples were used. There is a distinct gap between the upper and lower bounds, which agrees with the results in [3]. The capacity of the optimal simultaneous power and rate adaptation and the capacity of the optimal rate adaptation with constant transmit power scheme are basically indistinguishable at high SNR. It is noticeable at low SNR that the Monte Carlo simulation is tight to the lower bound. Similar results for the Monte Carlo simulation result were obtained for the other adaptive policies, but are omitted for clarity. Furthermore, the capacity performance of the truncated channel inversion with fixed rate is clearly suboptimal to the other schemes, as previously discussed.

Fig. 3.3 shows the probability of outage for the simultaneous optimal rate-power adaptation and for the truncated channel inversion schemes. In the former case, the optimal cut-off SNR was numerically found as in (3.20). In the latter case, the optimal cut-off SNR is the value that maximizes the capacity (3.31). However, this maximization occurs at the cost of increased probability of outage. These results are illustrated in Fig. 3.4, where the capacity per unit bandwidth is plotted as a function of the cut-off SNR γ_0^*, for $\bar{\gamma}_{s,d} = \bar{\gamma} = 5$, 10, 15 and 20 dB. The optimal cut off SNR γ_0^* that maximizes the capacity occurs at $\gamma_0 < \gamma_0^*$, as γ_0 is restricted between the interval [0,1]. This indicates that increased capacity occurs at the cost of some outage probability, as in Fig. 3.3. Furthermore, it can be seen that the lower bound on the outage probability is tight to the Monte Carlo simulation at low SNR and that the upper bound is tight to the Monte Carlo simulation at high SNR. For the case

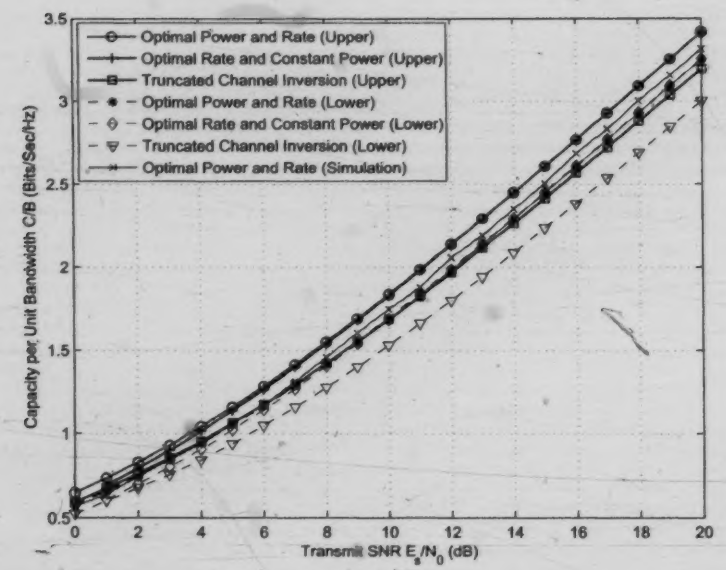

Fig. 3.2. Channel capacity comparison of adaptive schemes with i.i.d. Rayleigh fading channels.

of simultaneous optimal rate-power adaptation the Monte Carlo simulation was ran for 10^5 samples for SNR of 0 to 12 dB, 10^6 samples for SNR of 13 to 16 dB, and 10^7 samples for SNR of 17 to 20 dB. Similarly, for the case of truncated channel inversion the Monte Carlo simulation was ran for 10^6 samples for SNR of 0 to 12 dB, 10^7 samples for SNR of 13 to 20 dB.

For non-i.i.d. Rayleigh fading, the channel capacity with adaptive transmissions are plotted in Fig. 3.5. The average SNRs on the branches are as follows: $\bar{\gamma}_{s,1} = E_s/N_0$, $\bar{\gamma}_{s,2} = 0.8E_s/N_0$, $\bar{\gamma}_{1,d} = 0.3E_s/N_0$, $\bar{\gamma}_{2,d} = 0.56E_s/N_0$, and $\bar{\gamma}_{s,d} = 0.2E_s/N_0$. The results obtained are similar to the i.i.d. Rayleigh fading case, but, for this two-relay system, the gap between the truncated adaptive scheme and the optimal scheme is decreased. Also it was noticed that as the cooperative diversity increases (i.e., the number of relays increases) the difference in capacity of the adaptive channel inversion technique with respect to

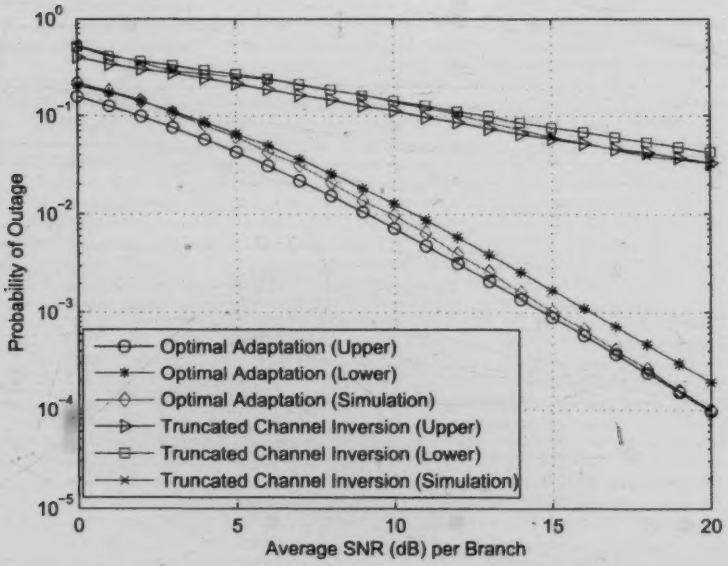

Fig. 3.3. Outage probability of adaptive schemes with i.i.d. Rayleigh fading channels.

the other adaptive techniques depreciates. The outage probability is plotted in Fig. 3.6.

3.5 Summary

This chapter has proposed the use of adaptive source transmission for the cooperative networks with fixed AF relay processing. To the best of the authors knowledge, this is the first time such source-adaptive relay networks have been analyzed. The Shannon capacity of the AF cooperative i.i.d. and non-i.i.d. Rayleigh fading channels with adaptive transmission are derived. The closed-form capacity bounds were found using a tight upper bound on the effective received SNR. The three adaptive techniques considered were: (i) optimal simultaneous power and rate adaptation; (ii) constant power with optimal rate

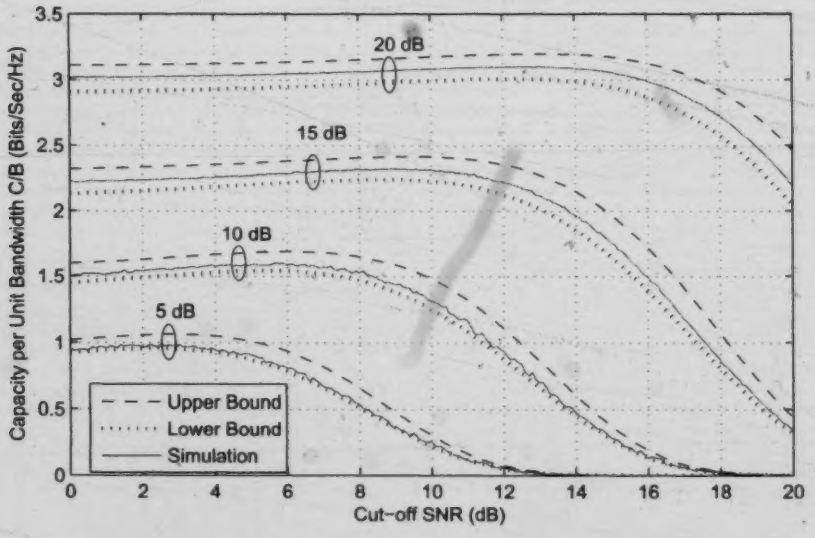

Fig. 3.4. Channel capacity versus cut-off SNR γ_0^* for $\bar{\gamma}_{s,d} = \bar{\gamma}$.

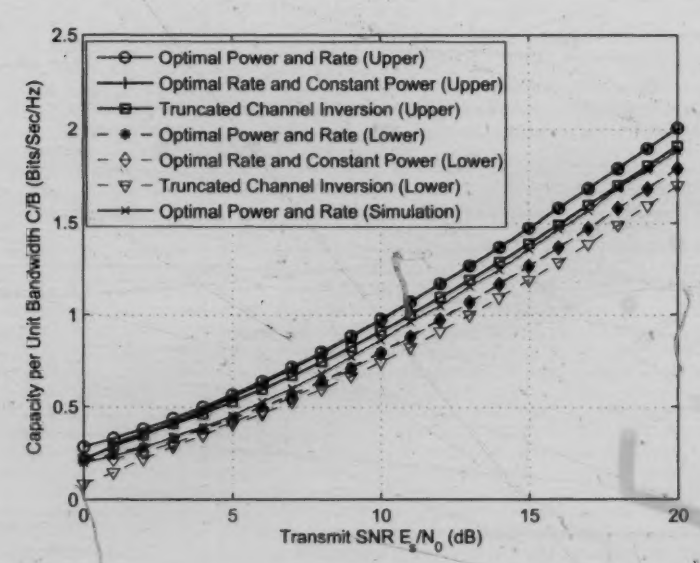
Optimal Power and Rate (Upper)
Optimal Rate and Constant Power (Upper)
Truncated Channel Inversion (Upper)
Optimal Power and Rate (Lower)
Optimal Rate and Constant Power (Lower)
Truncated Channel Inversion (Lower)
Optimal Power and Rate (Simulation)
Capacity per Unit Bandwidth C/B (Bits/Sec/Hz)
Transmit SNR Es/N0 (dB)

Fig. 3.5. Channel capacity comparison of adaptive schemes with non-i.i.d. Rayleigh fading channels.

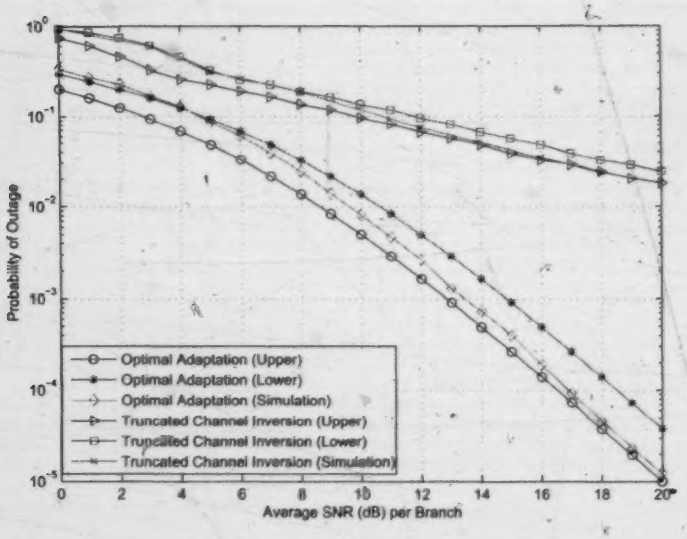

Fig. 3.6. Outage probability of adaptive schemes with non-i.i.d. Rayleigh fading channels.

adaptation; (iii) channel inversion with fixed rate. These capacity results represent achievable bounds for source-adaptive relay networks, and can be used as a bench mark to compare practical techniques to.

Chapter 4

Performance Analysis of Adaptive M-QAM for Rayleigh Fading Cooperative Systems

4.1 Introduction

IN THE PREVIOUS CHAPTER, adaptive transmission was analyzed for the Rayleigh fading AF cooperative networks[1]. However, no insight is given on how to achieve these capacity bounds. Although variable power, variable-rate adaptive schemes are known to be optimum in the sense they obtain the ergodic capacity, they have high implementation complexity. Thus, constant power with optimal rate adaptation scheme is a potential candidate for increasing capacity with reduced complexity [8,25]. Specifically, in [15] adaptive M-QAM for the classical communication systems is considered as a practical technique to realizing variable-rate fixed-power adaptive modulation.

Motivated by these observations, this chapter analyzes the performance of

[1] *A version of this chapter has been published in the proceedings of IEEE International Conference on Communications.*

the cooperative systems with constant power M-QAM adaptive rate transmission when the instantaneous BER is constrained to be below some threshold. In particular, the closed-form expressions for the outage probability, achievable spectral efficiency, and BER for the AF cooperative network in both i.i.d. and non-i.i.d. Rayleigh fading environments are derived. Note that these results provide a different perspective on the system implementation and analysis from the previous chapter, where the Shannon capacity for the non-regenerative cooperative system under adaptive transmissions for both i.i.d. and non-i.i.d. Rayleigh fading channels was derived.

This chapter is organized as follows. Section 4.2 presents the channel and system model. Analysis of adaptive M-QAM is conducted in Section 4.3. In Section 4.4 the numerical results are presented. A summary is given in Section 4.5.

4.2 Channel and System Model

The cooperative wireless network with adaptive M-QAM transmission is depicted in Fig. 4.1. However, the general channel and system model is the same as considered in Chapter 3, Section 3.2. Consequently, no discussion regarding the general cooperative system model will be given in this chapter.

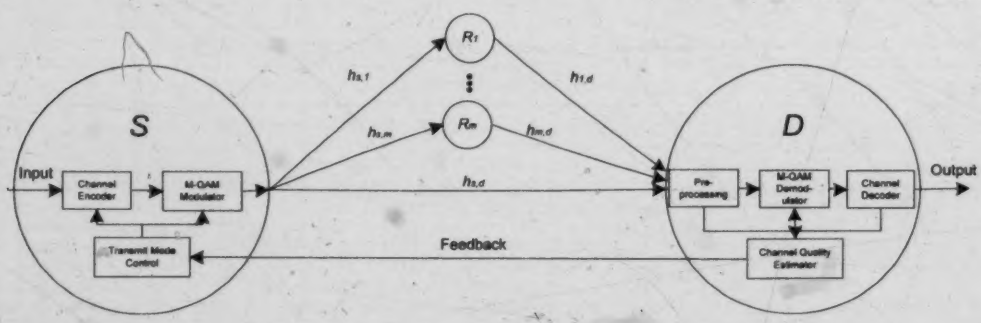

Fig. 4.1. Cooperative diversity wireless network with adaptive transmission.

4.3 Adaptive M-QAM Modulation

4.3.1 Adaptive Scheme

Among different adaptive transmission schemes, the constant-transmit-power and variable-rate scheme has many practical advantages. The destination needs only to calculate the total SNR and select the appropriate transmission rate and send this information back to the transmitter. This makes adaptive techniques based on adaptive M-QAM modulation such as those proposed in [2, 15] viable. For this reason, adaptive M-QAM is also considered in this chapter. The BER of a system which implements M-QAM modulation over an AWGN channel, with coherent detection and Gray coding can be approximated as [2, 15]

$$\mathrm{BER}(M, \gamma) \approx 0.2 \exp\left(\frac{-3\gamma}{2(M-1)}\right). \tag{4.1}$$

where again γ is the received SNR.

It is shown in [2] that the approximate BER (4.1) is indeed an upper bound on the exact BER for modulation order $M \geq 4$ and for BER $\leq 10^{-2}$. This approximation is used in [2, 15] and this work due to the fact that it is invertible, which yields nice closed-form solutions for determining the spectral efficiency, outage probability, and average BER. By inverting (4.1) the spectral efficiency of the continuous-rate M-QAM can be approximated as [2, 15]:

$$\frac{R}{B} = \log_2 M = \log_2\left(1 + \frac{3\gamma}{2K_0}\right), \tag{4.2}$$

where $K_0 = -\ln(5\mathrm{BER}_0)$ and BER_0 is the target BER. The spectral efficiency of (4.2) is achieved by using the adaptive continuous rate (ACR) M-QAM [11]. How ACR M-QAM works is the number of bits per symbol is varied depending on the instantaneous effective SNR γ. However, because of the practical limitation of ACR, adaptive discrete rate (ADR) M-QAM with constellation size $M_n = 2^n$ for n a positive integer, is implementable and is worth investigating.

The ADR M-QAM scheme performs as follows. The range of the effective received SNR is divided into $N+1$ regions. In each region, a specific constellation of size M_n is used. When the fading causes the effective SNR to fall into the nth region ($n = 0, 1, \ldots, N$), the constellation of size M_n is used for transmission. The partitioning of the effective received SNR depends on the desired BER level, BER_0. For instance, to have reliable communication which achieves a specific BER target of BER_0 using M_n-QAM, the region boundaries are set to the SNR required to achieve this desired performance, which can easily be shown to be [2]:

$$\begin{aligned} \gamma_1 &= [\text{erfc}^{-1}(2\text{BER}_0)]^2, \\ \gamma_n &= \tfrac{2}{3}K_0(2^n - 1); \quad n = 0, 2, 3, \ldots, N, \\ \gamma_{N+1} &= +\infty, \end{aligned} \tag{4.3}$$

where $\text{erfc}^{-1}()$ is the inverse complementary error function. This partition of the region boundaries is provided in [2], but presented here in Fig. 4.2 for clarity, for a desired BER_0 of 10^{-3}.

4.3.2 Outage Probability

The Case of I.I.D. Fading Channels

As no transmission occurs when the received SNR is below the smallest predetermined threshold γ_1, the probability of such an outage event is given by:

$$\begin{aligned} P_{\text{out}} &= P[\gamma_{ub} < \gamma_1] = \int_0^{\gamma_1} p_{\gamma_{ub}}(\gamma)d\gamma \\ &= 1 - \int_{\gamma_1}^{\infty} p_{\gamma_{ub}}(\gamma)d\gamma, \end{aligned} \tag{4.4}$$

where

$$\int_{\gamma_1}^{\infty} p_{\gamma_{ub}}(\gamma)d\gamma = \beta_0 e^{-\frac{\gamma_1}{\bar{\gamma}_{s,d}}} + e^{-\frac{2\gamma_1}{\bar{\gamma}}} \sum_{i=1}^{m} \beta_i \sum_{k=0}^{i-1} \frac{1}{k!} \left(\frac{2\gamma_1}{\bar{\gamma}}\right)^k \tag{4.5}$$

is established by using [17, eq. (3.351.2)]. Also, where the PDF $p_{\gamma_{ub}}(\gamma)$ is give as in (3.11). The constants β_0, β_i are as in (3.10) and $\bar{\gamma} = \mathbf{E}\{|h_{s,i}|^2\}E_s/N_0 = \mathbf{E}\{|h_{i,d}|^2\}E_s/N_0$, $\bar{\gamma}_{s,d} = \mathbf{E}\{|h_{s,d}|\}^2 E_s/N_0$.

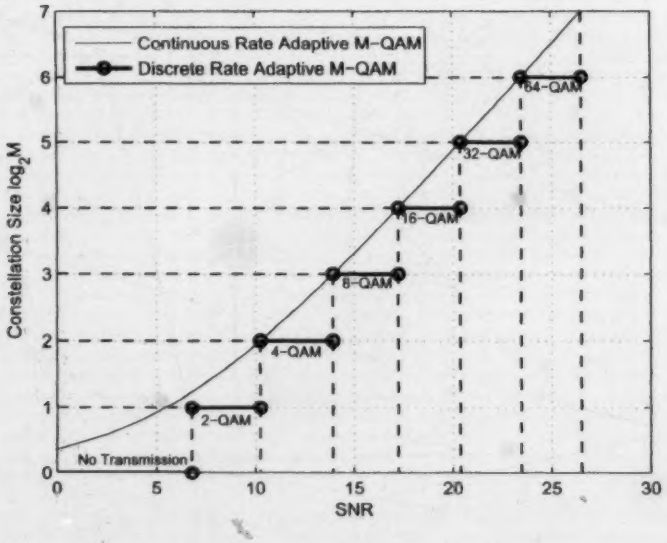

Fig. 4.2. Constellation size relative to the received SNR (dB).

The probability of outage is found by substituting (4.5) into (4.4), resulting in

$$P_{\text{out}} = 1 - \left[\beta_0 e^{-\frac{\gamma_1}{\bar{\gamma}_{s,d}}} + e^{-\frac{2\gamma_1}{\bar{\gamma}}} \sum_{i=1}^{m} \beta_i \sum_{k=0}^{i-1} \frac{1}{k!} \left(\frac{2\gamma_1}{\bar{\gamma}} \right)^k \right]. \tag{4.6}$$

The Case of Non-I.I.D. Fading Channels

In a similar fashion as the i.i.d case, the tail probability is

$$\int_{\gamma_1}^{\infty} p_{\gamma_{ub}}(\gamma) d\gamma = \widehat{\beta}_0 e^{-\frac{\gamma_1}{\bar{\gamma}_{s,d}}} + \sum_{i=1}^{m} \widehat{\beta}_i e^{-\frac{\gamma_1}{\tau_i}}. \tag{4.7}$$

Also, where the PDF $p_{\gamma_{ub}}(\gamma)$ is give as in (3.15). The constants $\widehat{\beta}_0$, $\widehat{\beta}_i$ are as in (3.14) and $\tau_i = \frac{\bar{\gamma}_{s,i}\bar{\gamma}_{i,d}}{\bar{\gamma}_{s,i}+\bar{\gamma}_{i,d}}$, $\bar{\gamma}_{s,i} = \mathbf{E}\{|h_{s,i}|^2\}E_s/N_0$ and $\bar{\gamma}_{i,d} = \mathbf{E}\{|h_{i,d}|^2\}E_s/N_0$, $\gamma_{s,d} = |h_{s,d}|^2 E_s/N_0$.

Likewise, the probability of outage is found by substituting (4.7) into (4.4) to give

$$P_{\text{out}} = 1 - \left[\widehat{\beta}_0 e^{-\frac{\gamma_1}{\bar{\gamma}_{s,d}}} + \sum_{i=1}^{m} \widehat{\beta}_i e^{-\frac{\gamma_1}{\tau_i}} \right]. \tag{4.8}$$

The analysis for the outage probability is the same as the case of optimal rate optimal power adaptation adaptation considered in Chapter 3 Section 3.3. However, γ_1 is the cutoff for ADR which satisfies the BER target level, while the cutoff γ_0 is the optimal cutoff defined by (3.17).

4.3.3 Achievable Spectral Efficiency

The Case of I.I.D. Fading Channels

The average spectral efficiency for ACR is found by integrating (4.2) over the PDF of the received SNR.

$$R_{\text{acr}} = \frac{B}{(m+1)\ln 2}\int_0^\infty \ln\left(1+\frac{3\gamma}{2K_0}\right) p_{\gamma_{sb}}(\gamma)d\gamma. \tag{4.9}$$

The factor $1/(m+1)$ accounts for the fact that the transmission process takes place in $(m+1)$ orthogonal channels or time-slots. Substituting (3.11) into (2.11), and making use of the integral $\mathcal{I}_n(\mu)$,

$$\begin{gathered}\mathcal{I}_n(\mu) = \int_0^\infty t^{n-1}\ln(1+t)e^{-\mu t}dt, \\ \mu > 0; \quad n = 1, 2, ...,\end{gathered} \tag{4.10}$$

which can be evaluated in a closed-form as in [1, eq. (78)], the closed-form expression for the achievable ACR spectral efficiency R_{acr} is

$$\begin{aligned}R_{\text{acr}} = \frac{B}{(m+1)\ln 2}\Bigg[&\frac{2K_0\beta_0}{3\bar{\gamma}_{s,d}}\mathcal{I}_1\left(\frac{2K_0}{3\bar{\gamma}_{s,d}}\right) \\ &+\sum_{i=1}^{m}\frac{\beta_i 4K_0(3\bar{\gamma})^{-i}}{(i-1)!}\mathcal{I}_i\left(\frac{4K_0}{3\bar{\gamma}}\right)\Bigg].\end{aligned} \tag{4.11}$$

For ADR the achievable average spectral efficiency is simply the sum of the data rates in each of the partition regions weighted by the probability of occurrence of each region and is given as follows:

$$R_{\text{adr}} = \frac{B}{(m+1)}\sum_{n=1}^{N} b_n\delta_n, \tag{4.12}$$

where $b_n = \log_2(M_n)$ corresponds to the data rate of the nth region. Furthermore, δ_n is the probability that the effective received SNR is in the nth partition region and is given as,

$$\delta_n = \int_{\gamma_n}^{\gamma_{n+1}} p_{\gamma_{ab}}(\gamma) d\gamma, \tag{4.13}$$

which evaluates to

$$\begin{aligned} \delta_n &= \beta_0 \left(e^{-\gamma_n/\gamma_{s,d}} - e^{-\gamma_{n+1}/\gamma_{s,d}} \right) \\ &+ \sum_{i=1}^{m} \beta_i \left(\mathcal{P}_i\left(\frac{2\gamma_n}{\bar{\gamma}}\right) - \mathcal{P}_i\left(\frac{2\gamma_{n+1}}{\bar{\gamma}}\right) \right), \end{aligned} \tag{4.14}$$

and where $\mathcal{P}_i(\cdot)$ denotes the Poisson distribution, defined as

$$\mathcal{P}_i(\mu) = e^{-\mu} \sum_{j=1}^{i-1} \frac{\mu^j}{j!}. \tag{4.15}$$

The Case of Non-I.I.D. Fading Channels

In a similar manner to the i.i.d fading channel, the closed-form expression for the average ACR spectral efficiency R_{acr} is

$$\begin{aligned} R_{\text{acr}} = \frac{B}{(m+1)\ln 2} \Bigg[& \frac{2K_0\widehat{\beta}_0}{3\bar{\gamma}_{s,d}} \mathcal{I}_1\left(\frac{2K_0}{3\bar{\gamma}_{s,d}}\right) \\ & + \sum_{i=1}^{m} \frac{2K_0\widehat{\beta}_i}{3\tau_i} \mathcal{I}_1\left(\frac{2K_0}{3\tau_i}\right) \Bigg]. \end{aligned} \tag{4.16}$$

The average ADR spectral efficiency R_{adr} for the non-i.i.d. fading channel can be found by using (4.12), where δ_n is,

$$\begin{aligned} \delta_n = & \widehat{\beta}_0 \left(e^{-\gamma_n/\gamma_{s,d}} - e^{-\gamma_{n+1}/\gamma_{s,d}} \right) \\ & + \sum_{i=1}^{m} \widehat{\beta}_i \left(e^{-\gamma_n/\tau_i} - e^{-\gamma_{n+1}/\tau_i} \right). \end{aligned} \tag{4.17}$$

4.3.4 Average Bit Error Rate

The Case of I.I.D. Fading Channels

As ACR M-QAM constantly meets the desired BER target, the BER analysis is not of interest as it is clearly fixed at the desired threshold. However, for

the ADR M-QAM the discrete partitions of the received SNR results in a conservative average BER. This results in the average BER_{adr} always being smaller then the target BER. The average BER_{adr} can easily be calculated as it is simply the ratio of the average number of bits in error divided by the total average number of transmitted bits,

$$\text{BER}_{\text{adr}} = \frac{\sum_{n=1}^{N} b_n \overline{\text{BER}}_n}{\sum_{n=1}^{N} b_n \delta_n}, \tag{4.18}$$

where

$$\overline{\text{BER}}_n = \int_{\gamma_n}^{\gamma_{n+1}} \text{BER}(M_n, \gamma) p_{\gamma_{nb}}(\gamma) d\gamma. \tag{4.19}$$

By substituting (3.11) and (4.1) into (4.19) the closed-form expression for the average BER for the nth region is

$$\begin{aligned}\overline{\text{BER}}_n = \frac{0.2\beta_0}{1+\bar{\gamma}_{s,d}c_n}\left(e^{-\gamma_n(\gamma_{s,d}^{-1}+c_n)} - e^{-\gamma_{n+1}(\gamma_{s,d}^{-1}+b_{n+1})}\right) \\ + \sum_{i=1}^{m} \frac{0.2\beta_i}{(1+0.5\bar{\gamma}c_n)^i}\Bigg(\mathcal{P}_i\left(\gamma_n(2\bar{\gamma}^{-1}+c_n)\right) \\ - \mathcal{P}_i\left(\gamma_{n+1}(2\bar{\gamma}^{-1}+c_n)\right)\Bigg),\end{aligned} \tag{4.20}$$

where

$$c_n = \frac{3}{2(2^n-1)}. \tag{4.21}$$

The Case of Non-I.I.D. Fading Channels

The average BER_{adr} for the non-i.i.d fading channel can be found by substituting in $\overline{\text{BER}}_n$ into (4.18), where

$$\begin{aligned}\overline{\text{BER}}_n = \frac{0.2\widehat{\beta}_0}{1+\bar{\gamma}_{s,d}c_n}\left(e^{-\gamma_n(\gamma_{s,d}^{-1}+c_n)} - e^{-\gamma_{n+1}(\gamma_{s,d}^{-1}+b_n)}\right) \\ + \sum_{i=1}^{m} \frac{0.2\beta_i}{1+c_n\tau_i}\left(e^{-\gamma_n(\tau_i^{-1}+c_n)} - e^{-\gamma_{n+1}(\tau+i^{-1}+b_{n+1})}\right).\end{aligned} \tag{4.22}$$

4.4 Numerical Results and Comparisons

In this section, numerical results for the outage probability, achievable spectral efficiency, and BER analysis for cooperative systems with adaptive M-QAM transmissions are presented. For all the numerical results containing to i.i.d. Rayleigh fading,the system model as in Chapter 3 (one relay ($m = 1$)), is considered. Although such a model is basic, the results of Section 4.3 can be used for any number of relays. The effects of path-loss or shadowing can also be taken into account readily. For the case of non-i.i.d. Rayleigh fading, all the numerical results are obtained with two relays ($m = 2$). The average SNR of the links are chosen arbitrarily as in Chapter 3 such that they represent a realistic model of a practical cooperative communication system. Specifically, they are as follows: $\bar{\gamma}_{s,1} = E_s/N_0$, $\bar{\gamma}_{s,2} = 0.8E_s/N_0$, $\bar{\gamma}_{1,d} = 0.3E_s/N_0$, $\bar{\gamma}_{2,d} = 0.56E_s/N_0$, and $\bar{\gamma}_{s,d} = 0.2E_s/N_0$.

Fig. 4.3 and Fig. 4.4 show the probability of outage (4.6) and (4.8) for the M-QAM rate adaptation under various target BER levels, for the i.i.d., and non-i.i.d. fading models, respectively. Note that the Monte Carlo simulation, with 10^5 samples, is also plotted to show the accuracy of the upper bound. It is quite clear to see the distinction between the diversity order for the $m = 1$ i.i.d. systems and the $m = 2$ non-i.i.d. systems. Also as expected, the diversity order of each system is independent of the BER target level.

In Fig. 4.5 the achievable spectral efficiency of ACR M-QAM (4.11) and ADR M-QAM (4.12) for the target BER level of $\text{BER}_0 = 10^{-3}$ for the i.i.d. fading model is plotted. The number of partition regions of the SNR vary from $3, 5, 7,$ and 9 to show the capacity for different number of regions. Also plotted for comparison is the Shannon capacity of the optimal rate and constant power cooperative system with i.i.d. Rayleigh fading found in Chapter 3, (3.29). Furthermore, the Monte Carlo simulation results are plotted where 5×10^3 samples were used for ACR and 10^4 samples were used for ADR. Similarly,

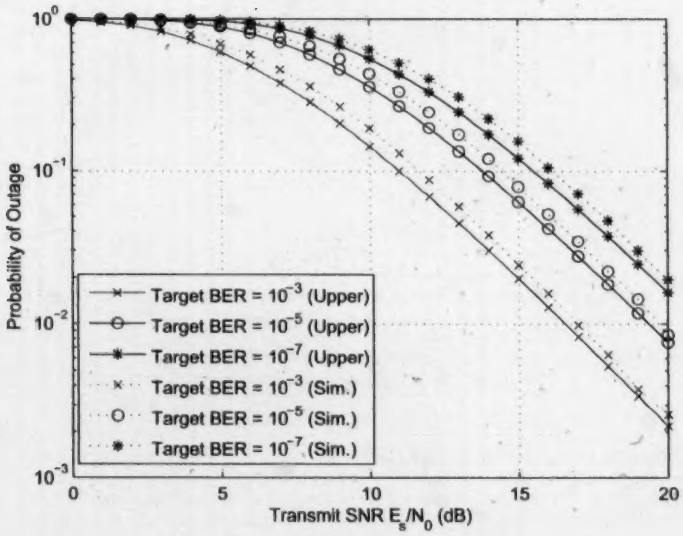
Probability of Outage
Transmit SNR E_s/N_0 (dB)
Target BER = 10^{-3} (Upper)
Target BER = 10^{-5} (Upper)
Target BER = 10^{-7} (Upper)
Target BER = 10^{-3} (Sim.)
Target BER = 10^{-5} (Sim.)
Target BER = 10^{-7} (Sim.)

Fig. 4.3. Outage probability of adaptive schemes with i.i.d. Rayleigh fading channels.

in Fig. 4.6 the achievable spectral efficiency of ACR M-QAM (4.11) and ADR M-QAM (4.12) for the target BER level of $\text{BER}_0 = 10^{-3}$ for the non-i.i.d. fading model is plotted and compared with the Shannon capacity of the optimal rate and constant power system previous plotted in Chapter 3, (3.30). Fig. 4.5 and Fig. 4.6 show that ACR M-QAM comes within 5 dB of the Shannon capacity limit. These figures are also similar in the performance of the achievable spectral efficiency of ADR M-QAM. For both cases of Rayleigh fading channels, ADR M-QAM suffers at least an additional 1.5 dB compared to the spectral efficiency of ACR M-QAM.

The BER (4.18) for the ADR M-QAM for both i.i.d. and non-i.i.d. Rayleigh fading model is plotted in Fig. 4.7 and Fig. 4.8 for the BER target of $\text{BER}_0 = 10^{-3}$. Since ACR M-QAM is instantaneous continuous adaptation, it always meets the BER target level. The average BER ADR M-QAM is always below the target level, this is because the switching thresholds are chosen such

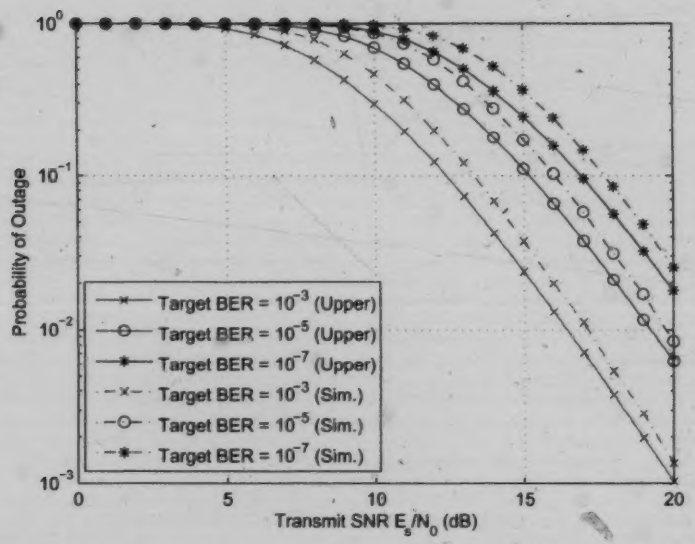
Probability of Outage
Transmit SNR E_s/N_0 (dB)
Target BER = 10^{-3} (Upper)
Target BER = 10^{-5} (Upper)
Target BER = 10^{-7} (Upper)
Target BER = 10^{-3} (Sim.)
Target BER = 10^{-5} (Sim.)
Target BER = 10^{-7} (Sim.)

Fig. 4.4. Outage probability of adaptive schemes with non-i.i.d. Rayleigh fading channels.

that the instantaneous BER is always guaranteed to be below the BER target level BER_0. This results in an inefficient use of spectrum (lower spectral efficiency) in terms of average BER. Although the switching thresholds can be optimized [8], this is not considered in this chapter as some applications do require to meet instantaneous BER levels.

4.5 Summary

This chapter investigated the performance analysis of adaptive M-QAM schemes for i.i.d. and non-i.i.d. Rayleigh fading cooperative channels. Specifically, the outage probability, achievable spectral efficiency, and BER were derived using an upper bound on the effective received SNR. The results indicate that ACR M-QAM approaches the Shannon capacity within 5 dB for both the i.i.d. and non-i.i.d Rayleigh fading models. However, the performance of ADR M-QAM

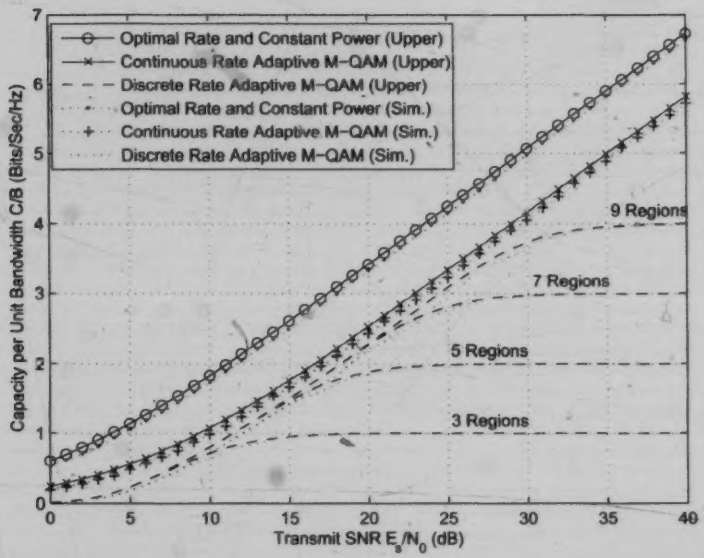

Fig. 4.5. Achievable rates of adaptive schemes with i.i.d. Rayleigh fading channels.

results in an additional penalty. The analysis is based on an upper bound on both the effective received SNR (3.5) and the approximate BER performance of M-QAM (4.1). Monte Carlo simulation results show the accuracy regarding the performance of the effective received SNR bound.

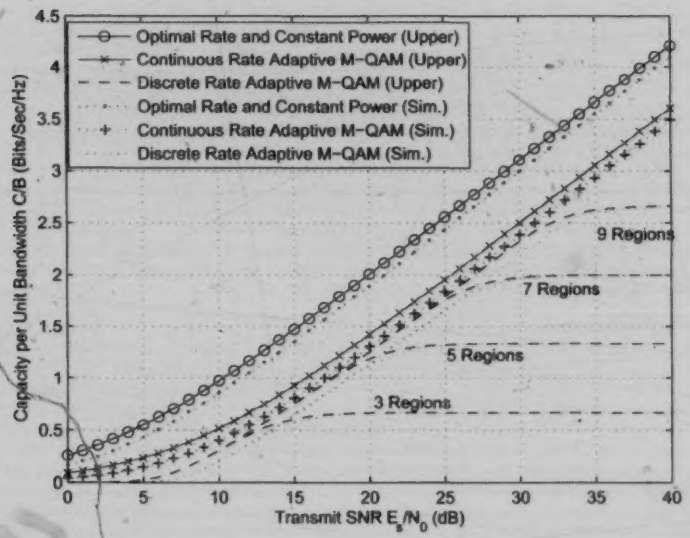
Optimal Rate and Constant Power (Upper)
Continuous Rate Adaptive M-QAM (Upper)
Discrete Rate Adaptive M-QAM (Upper)
Optimal Rate and Constant Power (Sim.)
Continuous Rate Adaptive M-QAM (Sim.)
Discrete Rate Adaptive M-QAM (Sim.)
9 Regions
7 Regions
5 Regions
3 Regions
Capacity per Unit Bandwidth C/B (Bits/Sec/Hz)
Transmit SNR E_s/N_0 (dB)

Fig. 4.6. Achievable rates of adaptive schemes with non-i.i.d. Rayleigh fading channels.

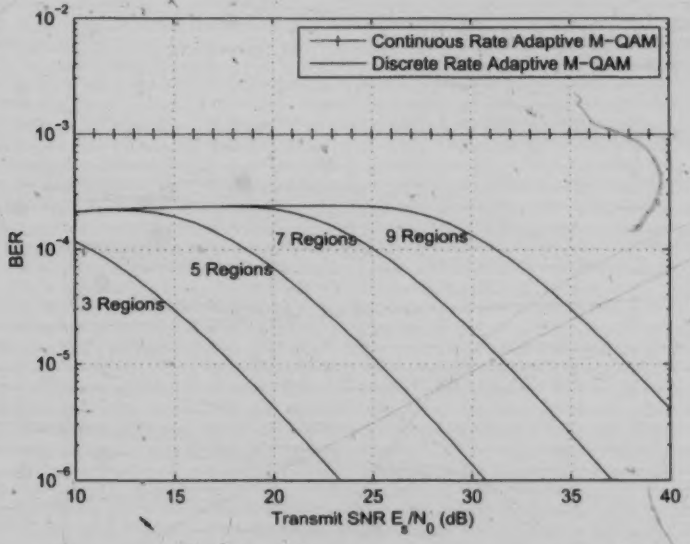

Fig. 4.7. Average BER for i.i.d. Rayleigh fading channels.

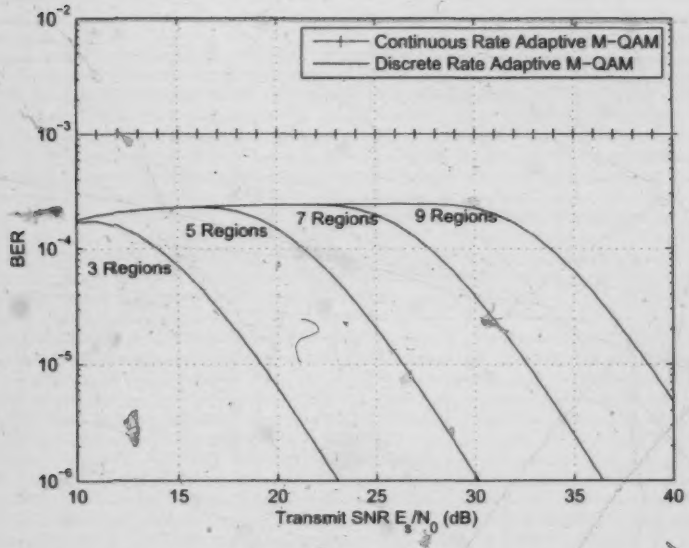

Fig. 4.8. Average BER for non-i.i.d. Rayleigh fading channels.

Chapter 5

Optimum Switching Adaptive M-QAM for Rayleigh Fading Cooperative Communication

5.1 Introduction

THE USE OF ADAPTIVE TRANSMISSION with an AF cooperative m relay network was proposed in Chapter 3[1]. The closed-form expressions are derived for the capacity of AF relaying over both i.i.d. Rayleigh fading and non-identical and independently distributed (non-i.i.d.) Rayleigh fading environments under these adaptive techniques. The capacity analysis is based on an accurate upper bound on the total effective SNR at the destination. In Chapter 4 the practical technique of adaptive M-QAM with fixed switching thresholds is applied to the cooperative network. Simultaneous to the work of this thesis, Hwang et. al [22] derive the performance analysis of adaptive M-QAM for a single incremental AF relay in Nakagami fading. In [22] the

[1] *A version of this chapter has been submitted to IEEE Transactions on Vehicular Technology.*

same upper bound on the SNR used in [35,36] is considered, and the spectral efficiency, BER, and outage probability are found.

Motivated by these observations, this chapter optimizes the switching thresholds for constant-power adaptive five-mode M-QAM transmission over an AF relay network. The optimization is based on the one-dimensional Lagrangian optimization method of [8]. The switching thresholds are optimized such that an average BER constraint is satisfied. The performance of optimal switching thresholds to that of fixed switching where an instantaneous BER constraint is enforced, is compared. The closed-form expressions for the outage probability, achievable spectral efficiency, and BER for the AF cooperative network in both i.i.d. and non-i.i.d. Rayleigh fading environments are computed and compared. Note that these results provide a different perspective on the system implementation and analysis from our previous results of Chapter 3 where the Shannon capacity for the non-regenerative cooperative system under adaptive transmissions for both i.i.d. and non-i.i.d. Rayleigh fading channels is derived. Furthermore, the results of this chapter are a more in depth and complete analysis of Chapter 4 where adaptive M-QAM with fixed switching is only considered.

This chapter is organized as follows. Section 5.2 presents the channel and system model. Analysis of adaptive M-QAM is conducted in Section 5.3. Section 5.4 discusses the optimization of the switching thresholds. The numerical results are presented in Section 5.5. A summary is given in Section 5.6.

5.2 Channel and System Model

The general channel and system model is the same as the one considered in Chapter 3, Section 3.2 and Chapter 4 Section 4.2.

TABLE 5.1

Five-Mode Adaptive M-QAM Parameters

SNR	$\gamma_0 \leq \gamma < \gamma_1$	$\gamma_1 \leq \gamma < \gamma_2$	$\gamma_2 \leq \gamma < \gamma_3$	$\gamma_3 \leq \gamma < \gamma_4$	$\gamma_4 \leq \gamma < \gamma_5$
n	0	1	2	3	4
M_n	0	2	4	16	64
b_n	0	1	2	4	6
mode	No Tx	BPSK	QPSK	16-QAM	64-QAM

5.3 Adaptive M-QAM

5.3.1 Five-Mode Adaptive M-QAM

The five-mode M-QAM scheme performs slightly different the adaptive M-QAM considered in Chapter 4, as only square QAM constellation are used five-mode transmission. Similarly to the Chapter 4, the range of the effective received SNR is divided into $N + 1$ regions, partitioned by a set of switching thresholds. In each region, a specific constellation of size M_n is used. When the fading causes the effective SNR to fall into the nth region ($n = 0, 1, \ldots, N$) and the constellation of size M_n is used for transmission. For all analysis in this chapter, five-mode adaptive M-QAM is considered as it has been well studied by researchers [8]. The parameters for five-mode adaptive M-QAM are given in Table 5.1, where again γ is the instantaneous received SNR, b_n is the number of bits per a transmitted symbol, $\gamma_0 = 0$ and $\gamma_5 = \infty$.

5.3.2 Outage Probability

The outage probability of the system can be found identically to that of Chapter 4. Please refer back to Section 4.3.2 for the complete analysis.

5.3.3 Achievable Spectral Efficiency

The achievable spectral efficiency of the system can be found identically to that of Chapter 4. Please refer back to Section 4.3.3 for the complete analysis.

5.3.4 Average Bit Error Rate

The Case of I.I.D. Fading Channels

The average BER of the system can be found similarly to that of Chapter 4, Section 4.3.4. The exception is that in Chapter 4 the BER was approximated as in (4.1). In this section it will be seen that a tighter approximation is used for the BER. For M-QAM with discrete partitions the average BER_{adr} can easily be calculated as it is simply the ratio of the average number of bits in error divided by the total average number of transmitted bits,

$$\text{BER}_{\text{adr}} = \frac{\sum_{n=1}^{N} b_n P_{n,QAM}}{\sum_{n=1}^{N} b_n \delta_n}, \tag{5.1}$$

where $P_{n,QAM}$ is the average BER in a specific SNR region of $[\gamma_n, \gamma_{n+1}]$ and can be represented as

$$P_{n,QAM} = \int_{\gamma_n}^{\gamma_{n+1}} p_{m_n,QAM}(\gamma) p_{\gamma_{\text{sb}}}(\gamma) d\gamma, \tag{5.2}$$

where $p_{m_n,QAM}(\gamma)$ is the BER of a system which implements square M-QAM over an AWGN channel, with coherent detection and Gray coding as in [8]

$$p_{m_n,QAM}(\gamma) = \sum_{l} A_l Q(\sqrt{a_l \gamma}), \tag{5.3}$$

where $Q(\cdot)$ is the standard Gaussian Q-function defined as $Q(x) = \frac{1}{\sqrt{2\pi}} \int_x^\infty \exp(-\lambda^2/2) d\lambda$, γ is the received SNR, and A_l and a_l are some constants shown in Table 5.2.

After some mathematical manipulation as shown in the Appendix, $P_{n,QAM}$

TABLE 5.2

M-QAM BER Parameters

M_n	Mode	$\{(A_l, a_l)\}$
2	BPSK	$\{(1,2)\}$
4	QPSK	$\{(1,1)\}$
16	16-QAM	$\left\{(\frac{3}{4},\frac{1^2}{5}),(\frac{2}{4},\frac{3^2}{5}),(-\frac{1}{4},\frac{5^2}{5})\right\}$
64	64-QAM	$\left\{(\frac{7}{12},\frac{1^2}{21}),(\frac{6}{12},\frac{3^2}{21}),(-\frac{1}{12},\frac{5^2}{21}),(\frac{1}{12},\frac{9^2}{21}),(-\frac{1}{12},\frac{13^2}{21})\right\}$

can be written as

$$
\begin{aligned}
P_{n,QAM} \;=\; & \beta_0 \sum_l A_l \Bigg[Q(\sqrt{a_l\gamma}) \left[1 - e^{-\frac{\gamma}{\bar{\gamma}_{s,d}}}\right] \Bigg|_{\gamma_n}^{\gamma_{n+1}} \\
& -\frac{1}{2}\Bigg\{ (\pi)^{-0.5}\Gamma(0.5, \frac{\gamma a_l}{2})\Big|_{\gamma_n}^{\gamma_{n+1}} \\
& -\sqrt{\frac{a_l}{2\pi}}(a_l/2+\bar{\gamma}_{s,d}^{-1})^{-0.5}\Gamma(0.5,(a_l/2+\bar{\gamma}_{s,d}^{-1})\gamma)\Big|_{\gamma_n}^{\gamma_{n+1}} \Bigg\}\Bigg] \\
& + \sum_l A_l \sum_{i=1}^{m} \beta_i \Bigg[Q(\sqrt{a_l\gamma}) \left(1 - e^{-\frac{\gamma}{(0.5\bar{\gamma})}} \sum_{r=0}^{i-1} \frac{(2\gamma/\bar{\gamma})^r}{r!}\right) \Bigg|_{\gamma_n}^{\gamma_{n+1}} \\
& -\frac{1}{2}\Bigg\{ (\pi)^{-0.5}\Gamma(0.5, \frac{\gamma a_l}{2})\Big|_{\gamma_n}^{\gamma_{n+1}} \\
& -\sqrt{\frac{a_l}{2\pi}} \sum_{r=0}^{i-1} \frac{(0.5\bar{\gamma})^{-r}}{r!}(a_l/2+2/\bar{\gamma})^{-r-0.5}\Gamma(r+0.5,(a_l/2+2/\bar{\gamma})\gamma)\Big|_{\gamma_n}^{\gamma_{n+1}} \Bigg\}\Bigg].
\end{aligned}
\tag{5.4}
$$

The Case of Non-I.I.D. Fading Channels

In a similar manner to the i.i.d fading channel the average BER can be computed as in (5.1) where

$$
\begin{aligned}
P_{n,QAM} \;=\; & \widehat{\beta}_0 \sum_{l} A_l \Bigg[Q(\sqrt{a_l\gamma}) \left[1 - e^{-\frac{\gamma}{\bar{\gamma}_{s,d}}}\right] \Bigg|_{\gamma_n}^{\gamma_{n+1}} \\
& -\frac{1}{2}\Bigg\{ (\pi)^{-0.5}\Gamma(0.5, \frac{\gamma a_l}{2})\Big|_{\gamma_n}^{\gamma_{n+1}} \\
& -\sqrt{\frac{a_l}{2\pi}}(a_l/2 + \bar{\gamma}_{s,d}^{-1})^{-0.5}\Gamma(0.5, (a_l/2 + \bar{\gamma}_{s,d}^{-1})\gamma)\Big|_{\gamma_n}^{\gamma_{n+1}} \Bigg\}\Bigg] \\
& + \sum_{l} A_l \sum_{i=1}^{m} \widehat{\beta}_i \Bigg[Q(\sqrt{a_l\gamma}) \left[1 - e^{-\frac{\gamma}{\tau_i}}\right] \Bigg|_{\gamma_n}^{\gamma_{n+1}} \\
& -\frac{1}{2}\Bigg\{ (\pi)^{-0.5}\Gamma(0.5, \frac{\gamma a_l}{2})\Big|_{\gamma_n}^{\gamma_{n+1}} \\
& -\sqrt{\frac{a_l}{2\pi}}(a_l/2 + \tau_i^{-1})^{-0.5}\Gamma(0.5, (a_l/2 + \tau_i^{-1})\gamma)\Big|_{\gamma_n}^{\gamma_{n+1}} \Bigg\}\Bigg].
\end{aligned}
\tag{5.5}
$$

5.4 Switching Thresholds

5.4.1 Fixed Switching Thresholds

With fix partitioning to have reliable communication which achieves a specific BER target of BER_0 using M_n-QAM, the switching thresholds or region boundaries are set to the SNR required to achieve this desired performance, are [2]:

$$
\begin{aligned}
&\gamma_1 = [\mathrm{erfc}^{-1}(2\mathrm{BER}_0)]^2, \\
&\gamma_n = \tfrac{2}{3}K_0(M_n - 1); \quad n = 0, 2, 3, \ldots, N, \\
&\gamma_{N+1} = +\infty
\end{aligned}
\tag{5.6}
$$

where $\mathrm{efrc}^{-1}()$ is the inverse complementary error function and $K_0 = -\ln(5\mathrm{BER}_0)$. This partition of the switching thresholds is shown in Fig. 5.1 for five-mode adaptive M-QAM, for a desired BER_0 of 10^{-3}. However, this technique only

limits the peak instantaneous BER and is an inefficient use of spectrum or in other words results in a lower spectral efficiency. It will be shown next, that the switching thresholds can be optimized so that the average BER always meets the desired BER threshold.

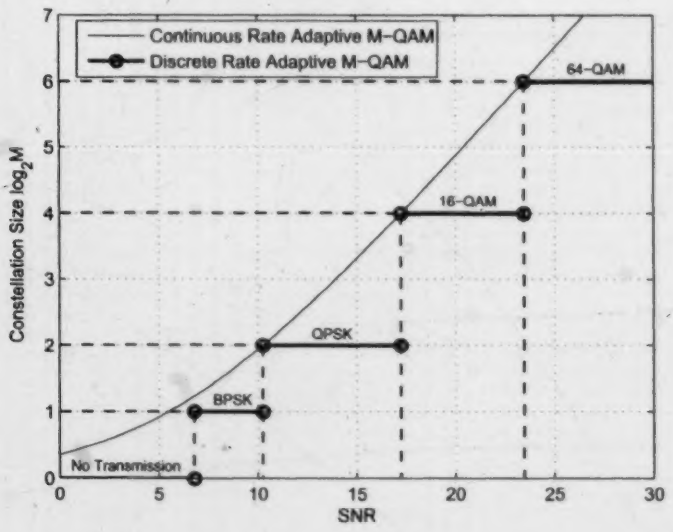

Fig. 5.1. Constellation size relative to the received SNR (dB).

5.4.2 Optimum Switching Thresholds

Subject to a constraint on the average BER, the switching thresholds can be optimized to maximize the throughput. For instance, in [2] the switching thresholds are chosen as in (5.6), which are designed for an AWGN channel. Optimization of the switching thresholds can be performed so that the average BER always meets the desired BER threshold. That is, one designs a set of switching thresholds, denoted as $\boldsymbol{s} = \{\gamma_n | n = 0, 1, \ldots, N\}$, such that the average throughput $R_{\text{adr}}(\bar{\gamma}, \boldsymbol{s})$ is maximized, under the constraint that the average BER equals the desired BER target, $\text{BER}_{\text{adr}} = \text{BER}_0$. The Lagrangian

optimization technique for deriving the globally optimized modulation-mode switching thresholds can then be used [8]. The optimization problem required is only one-dimensional and can be performed off-line so it does not add a layer of complexity to the system.

Lagrangian optimization problem formulation:
Maximize the *objective function* $R_{adr}(\bar{\gamma}, \boldsymbol{s})$ as given in (4.12), where it is *Constrained* by $\text{BER}_{adr} = \text{BER}_0$ as given in (5.1).

$$\max_{\boldsymbol{s}} \quad \sum_{n=1}^{N} b_n \delta_n \tag{5.7}$$

$$\text{subject to:} \quad \sum_{n=1}^{N} b_n P_{n,QAM} = \text{BER}_0 \sum_{n=1}^{N} b_n \delta_n \tag{5.8}$$

Furthermore, assuming that the switching thresholds are ordered

$$\gamma_n \leq \gamma_{n+1} \tag{5.9}$$

also $\gamma_0 = 0$ and $\gamma_N = \infty$ the optimization problem consists of $N-1$ independent variables, and hence a $N-1$ dimensional optimization problem, as discussed in [8]. Using a modified objective function it is shown in [8] that this problem can be formulated as a one-dimensional Lagrangian optimization problem. The details to this optimization problem can be found in [8], and only the important results are summarized here.

The first step is to identify that γ_n ($n \geq 1$) are all dependent upon γ_1 and is shown in [8], that for five-mode adaptive M-QAM that the switching

thresholds $\boldsymbol{s}$ are constrained by the following equations

$$y_k(\gamma_k) = y_1(\gamma_1); \text{for k=2,3,...,N}, \tag{5.10}$$

$$y_1(\gamma_1) = p_{2,QAM}(\gamma_1), \tag{5.11}$$

$$y_2(\gamma_2) = 2p_{4,QAM}(\gamma_2) - p_{2,QAM}(\gamma_2), \tag{5.12}$$

$$y_3(\gamma_3) = 2p_{16,QAM}(\gamma_3) - p_{4,QAM}(\gamma_3), \tag{5.13}$$

$$y_4(\gamma_4) = 3p_{64,QAM}(\gamma_4) - 2p_{16,QAM}(\gamma_4), \tag{5.14}$$

and are plotted in [8] and illustrated here for clarity in Fig. 5.2.

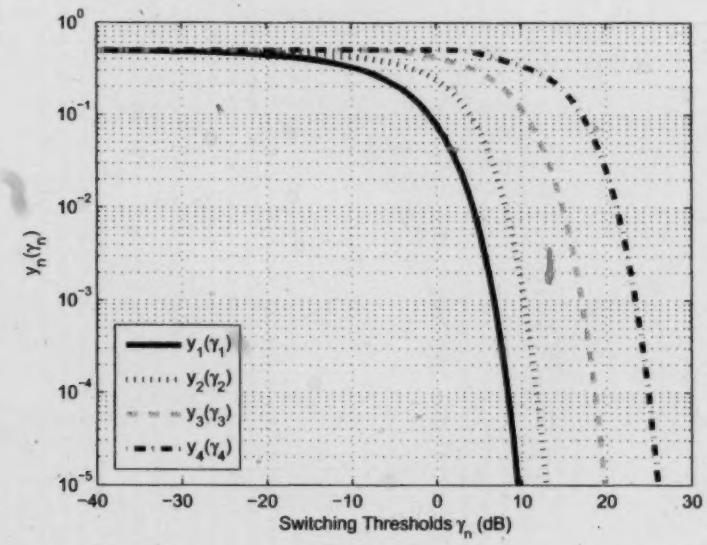

Fig. 5.2. Switching level constraint relationship.

Given (5.10-5.14) the switching thresholds $\gamma_2, \gamma_3, \gamma_4$ can be found in terms of γ_1. That is, $\gamma_2 = y_2^{-1}(y_1(\gamma_1)), \gamma_3 = y_3^{-1}(y_1(\gamma_1))$, and $\gamma_4 = y_4^{-1}(y_1(\gamma_1))$. The corresponding values of $\gamma_2, \gamma_3, \gamma_4$ can be found numerically in terms of γ_1 and are provided in [8] but presented here for clarity in Fig. 5.3.

Since all the switching thresholds depend on the first threshold γ_1, the optimization problem is only concerned with finding the optimal value for γ_1.

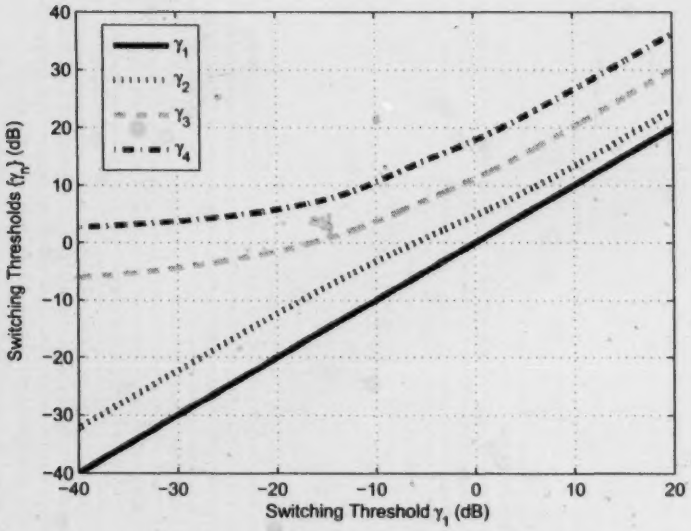

Fig. 5.3. Switching thresholds as a function of γ_1.

For a given target BER of BER_0, and the PDF of the effective SNR (3.11) or (3.15) the optimal value for γ_1 can be solved. Thus, the optimization problem is a simple one-dimensional root-finding problem where the constrain function is given as in [8],

$$Y(\bar{\gamma}; \boldsymbol{s}(\gamma_1)) = \sum_{n=1}^{N} b_n P_{n,QAM} - \text{BER}_0 \sum_{n=1}^{N} b_n \delta_n = 0. \tag{5.15}$$

Clearly, it is noticeable the relationship between $Y(\bar{\gamma}; \boldsymbol{s}(\gamma_1))$ (5.15) and (5.8). Furthermore, the first term of $Y(\bar{\gamma}; \boldsymbol{s}(\gamma_1))$ can intuitively be thought of as the sum of the BER in each mode weighed by the average throughput of each mode [8]. While the second term of $Y(\bar{\gamma}; \boldsymbol{s}(\gamma_1))$, is average throughput weighed by the desired BER threshold. This means that, $Y(\bar{\gamma}; \boldsymbol{s}(\gamma_1))$ (5.15) represents the difference between the average BER and the desired BER, BER_0. Consequently, the problem is to find the solution to $Y(\bar{\gamma}; \boldsymbol{s}(\gamma_1)) = 0$, when it exists.

5.5 Numerical Results and Comparisons

This section presents, the numerical results for the achievable spectral efficiency, the outage probability, and the BER for cooperative systems with adaptive five-mode M-QAM transmissions. Optimal switching thresholds and fixed switching thresholds are computed and compared. For i.i.d. and non-i.i.d Rayleigh fading, the system with one relay, $m = 1$ and two relays, $m = 2$ is considered, respectively. However, the results of Section 5.3 and 5.4 can be used for any number of relays. As before, this is the same system model considered in Chapter 3 and 4.

In Fig. 5.4 the constraint function (5.15) is plotted for i.i.d. Rayleigh fading with one relay, $m = 1$ where $\bar{\gamma}_{s,d} = \bar{\gamma}$. Adaptive five-mode M-QAM is considered where the average transmit SNR is set to 20dB. $Y(\bar{\gamma}; \boldsymbol{s}(\gamma_1))$ is plotted for several target BER thresholds $BER_0 = \{10^{-2}, 10^{-3}, 10^{-4}, 10^{-6}\}$ to illustrate the solution to $Y(\bar{\gamma}; \boldsymbol{s}(\gamma_1)) = 0$.

Fig. 5.5 shows the switching thresholds for both the Lagrangian optimization technique and the fixed switching thresholds as given in (5.6) for adaptive five-mode M-QAM for i.i.d. Rayleigh fading with one relay, where the target BER is set to $\text{BER}_0 = 10^{-3}$. It can be seen that there is an avalanche SNR of $\bar{\gamma}_a \sim 27.5$dB, where all of the switching thresholds avalanche to zero. This occurs when the BER of highest order modulation mode equals to the target BER threshold, $P_4, QAM(\bar{\gamma}_a) = \text{BER}_0$. Once this avalanche SNR is reached, rate adaption is abandoned and only the highest order modulation mode is used for transmission. Furthermore, it is worth mentioning that a unique solution to (5.15) $Y(\bar{\gamma}; \boldsymbol{s}(\gamma_1)) = 0$ exists as long as the transmit SNR is less than the avalanche SNR, $\bar{\gamma} < \bar{\gamma}_a$.

For optimal switching and for fixed switching the achievable spectral efficiency is plotted in Fig. 5.6 for adaptive five-mode M-QAM for i.i.d. Rayleigh fading with one relay, where the target BER is set to $\text{BER}_0 = 10^{-3}$. It

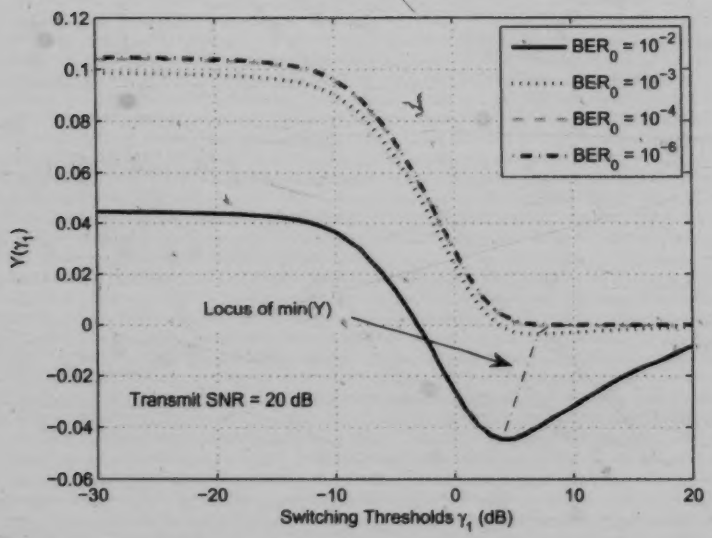

Fig. 5.4. Constraint function $Y(\bar{\gamma}; \boldsymbol{s}(\gamma_1))$ for i.i.d. Rayleigh fading with $m = 1$ relay.

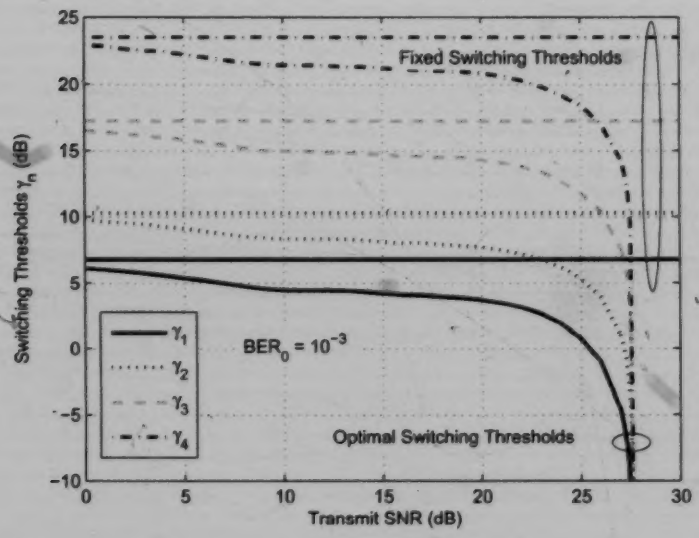

Fig. 5.5. Switching thresholds for i.i.d. Rayleigh fading with $m = 1$ relay.

can be seen that optimal switching compared to fixed switching results in a $\sim 2 - 2.5$dB improvement of the required transmit SNR to achieve a specific average throughput. Monte Carlo simulation with 10^4 samples is also plotted along with the upper bound analysis. It can be seen that upper bound is fairly tight and is within 1dB of the simulation results, this is as expected as a similar results occurs in [3, 23] and the previous two chapters of this thesis. Furthermore, in Fig. 5.7 the outage probability is plotted along with Monte Carlo simulation with 10^5 samples. Similarly, there is an improvement in required transmit SNR for a specific outage probability. For instance, at a probability of outage of 10^{-2} there is $\sim$ 2dB improvement in SNR. The BER is plotted in Fig. 5.8. It is clear that the optimal switching always meets the desired BER threshold of $\text{BER}_0 = 10^{-3}$ until the avalanche SNR is reached where it then has the error probability equal to the error probability for 64-QAM. Also, the BER for fixed switching results in a conservative average BER that is always below the BER target $\text{BER}_0 = 10^{-3}$. Semi-analytical simulation results with 10^3 samples for the BER are also plotted, that is (5.3) is used to calculate the instantaneous BER, while the channel model is statistically simulated. The simulation results for the BER are fairly tight to the analytical results, and further substantiate the validity of using the upper bound of (3.5).

For non-i.i.d. Rayleigh fading, Fig. 5.9 shows the switching thresholds for both the Lagrangian optimization technique and the fixed switching thresholds as given in (5.6) for adaptive five-mode M-QAM with two relay, where the target BER is set to $\text{BER}_0 = 10^{-3}$. The average SNRs on the branches are as follows: $\bar{\gamma}_{s,1} = E_s/N_0$, $\bar{\gamma}_{s,2} = 0.8E_s/N_0$, $\bar{\gamma}_{1,d} = 0.3E_s/N_0$, $\bar{\gamma}_{2,d} = 0.56E_s/N_0$, and $\bar{\gamma}_{s,d} = 0.2E_s/N_0$. The results obtained are similar to the i.i.d. Rayleigh fading case, and the avalanche SNR $\bar{\gamma}_a \sim 27.5$dB. Similarly to the i.i.d. case the spectral efficiency, outage probability, and BER are plotted in Fig.'s 5.10, 5.11, and 5.12, respectively.

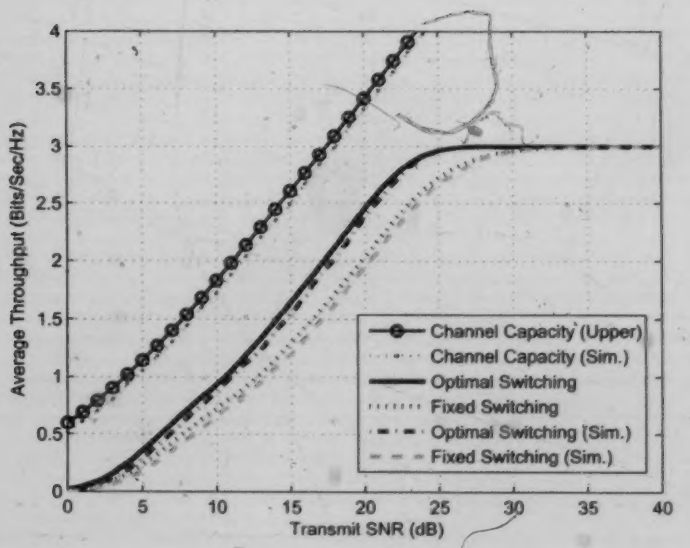

Fig. 5.6. Achievable rate for i.i.d. Rayleigh fading with $m = 1$ relay.

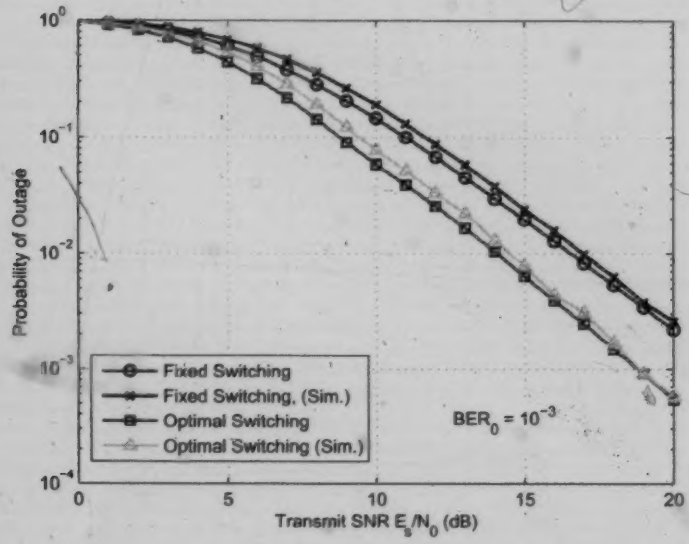

Fig. 5.7. Outage probability for i.i.d. Rayleigh fading with $m = 1$ relay.

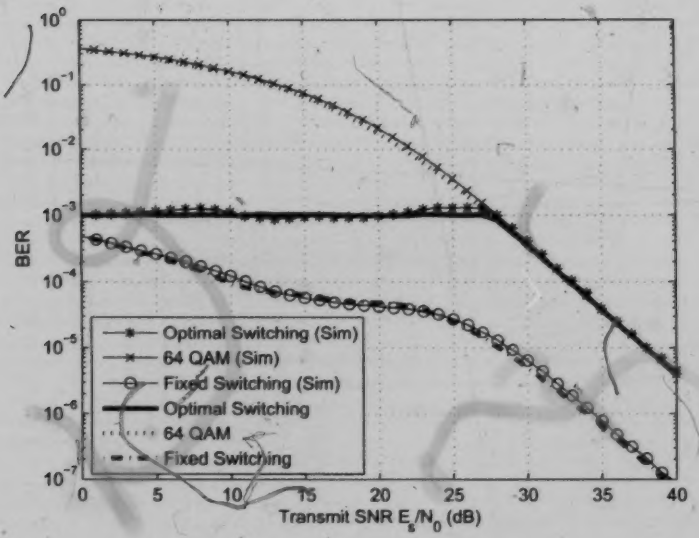

Fig. 5.8. Average bit error rate for i.i.d. Rayleigh fading with $m = 1$ relay.

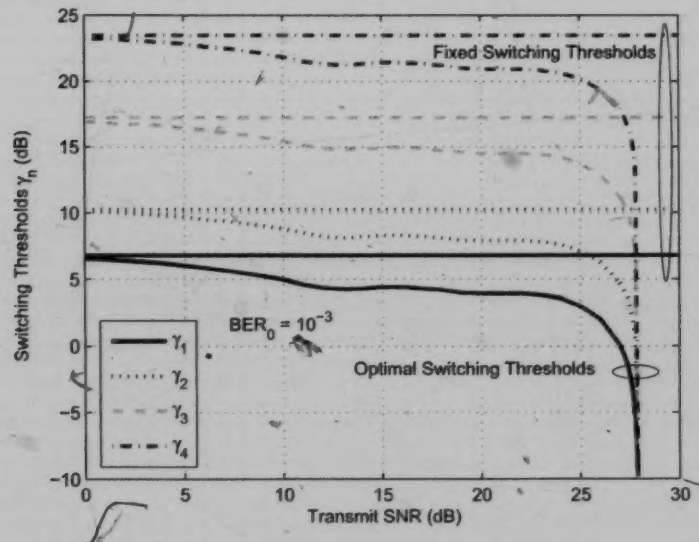

Fig. 5.9. Switching thresholds for non-i.i.d. Rayleigh fading with $m = 2$ relays.

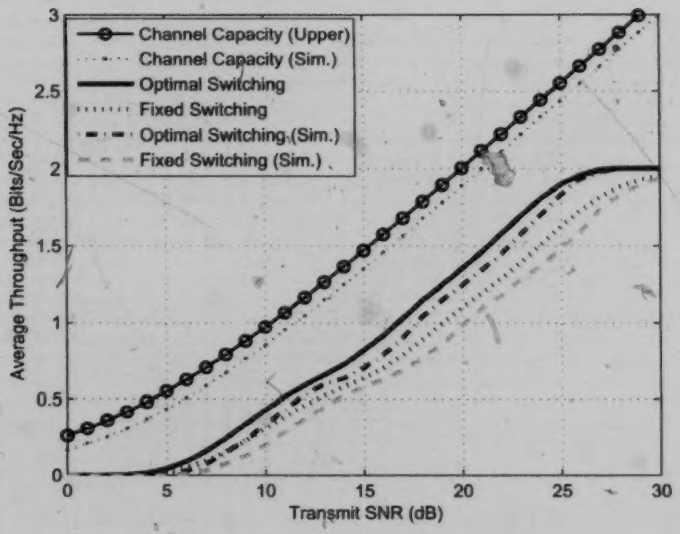

Fig. 5.10. Achievable rate for non-i.i.d. Rayleigh fading with $m = 2$ relays.

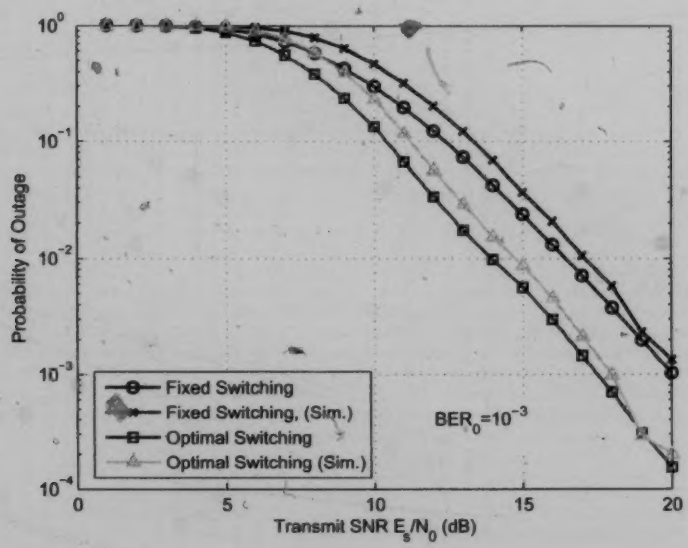

Fig. 5.11. Outage probability for non-i.i.d. Rayleigh fading with $m = 2$ relays.

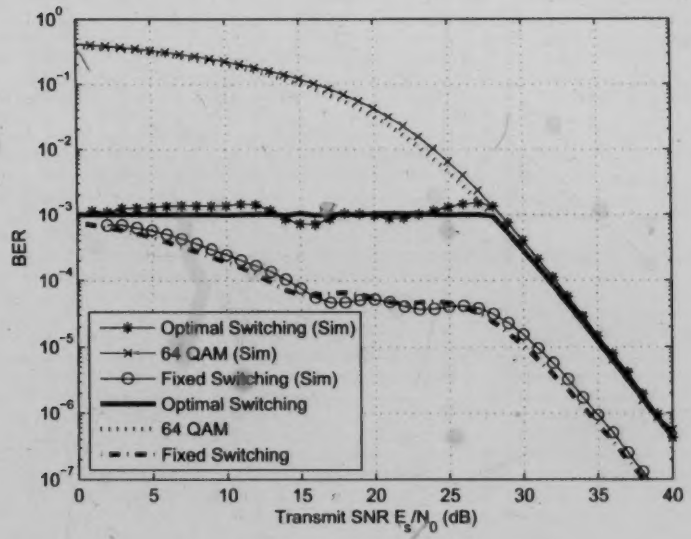

Fig. 5.12. Average bit error rate for non-i.i.d. Rayleigh fading with $m = 2$ relays.

5.6 Summary

This chapter investigated optimum and fixed switching adaptive M-QAM schemes for i.i.d. and non-i.i.d. Rayleigh fading cooperative channels. The Lagrangian optimization technique was applied to find the optimal switching thresholds. The performance of optimum and fixed switching adaptive M-QAM was analyzed and compared. Specifically, the outage probability, achievable spectral efficiency, and BER were derived. The analysis relied on using an upper bound on the effective received SNR (3.5). Monte Carlo simulation results show the accuracy regarding the performance of the effective received SNR bound. Moreover, a tight upper bound [8] on the BER performance of M-QAM (5.3) is used for the optimizing the switching thresholds. The results indicate that for a specific average throughput optimum switching thresholds gain 2.5 dB compared to fixed switching. Furthermore, the spectral

efficiency of adaptive five-mode M-QAM with optimized switching was compared to the theoretical Shannon channel capacity derived in Chapter 3 and approaches this fundamental limit within ~ 6 dB.

Chapter 6

Conclusions and Future Work

6.1 Conclusions

THIS THESIS HAS ANALYZED the AF cooperative network under adaptive transmission protocols. First the network capacity was derived under three adaptive protocols. Second, the practical technique of adaptive M-QAM with fixed switching levels was applied. Finally, the switching levels of adaptive M-QAM were optimized to increase the spectral efficiency.

Chapter 1 provides the motivations for the problems considered and analyzed in this thesis. The contributions of the thesis are briefly presented along with an outline.

Chapter 2 discuses the preliminary work and background of cooperative communication systems. A brief review of the previous research along with the benefits of cooperative communication are discussed. Furthermore, the transmission technique of adaptive modulation is discussed. A brief overview of the adaptive protocols (i) optimal simultaneous power and rate adaptation; (ii) constant power with optimal rate adaptation; (iii) channel inversion with fixed rate, are presented and the capacity of each technique is formulated.

Chapter 3 ties the techniques of adaptive modulation and cooperative com-

munication together and presents the combined system model. The motivation to consider the combined model is reassured with a discussion of the current literature. In fact, the proposed system model of combining adaptive transmission with cooperative communications is original as it has not been studied in the existing literature. The capacity of the system is derived using a tight upper bound. The capacity and outage probability of the different adaptive policies are compared and it is shown that channel inversion suffers sever penalties compared to the other adaptive policies.

Chapter 4 applies the technique of adaptive M-QAM to the cooperative communication system. Continuous rate adaption and discrete rate adaptation with fixed switching levels is considered. The spectral efficiency of the adaptive M-QAM cooperative network is compared to the theoretical channel capacity of the system previously derived in Chapter 3. It was seen that discrete rate adaptation suffers a small loss in capacity compared to the unpractical continuous rate adaption, while both come with in a constant gap of the Shannon capacity.

Chapter 5 optimizes the switching levels for five-mode adaptive M-QAM for cooperative communication. The optimization is achieved by placing a constraint on the desired average BER. It was observed that optimum switching levels result in over 2 dB gain in compared to fix switching. The outage probability and BER plotted and compared.

6.2 Future Work

This thesis is the first of its kind in adaptive transmission for cooperative communication systems, and opens up a large number of research problems. For instance the work of thesis can be extended for other fading channel models such as Nakagami or Rician fading. Other cooperative protocols and network could also be considered, such as DF relays. Furthermore, relay selection where

only a subset of the relays re-transmits to the destination could be analyzed. Distribution space time coding could also be considered for such a network. Moreover, the technique of source adaptive transmission could be applied to many of the node resource allocation problems.

Appendix A

Derivation for $P_{n,QAM}$

A.1 The Case of I.I.D. Fading Channels

The BER for square QAM with gray coding over an AWGN channel can be represented as [8]:

$$p_{m_n,QAM}(\gamma) = \sum_l A_l Q(\sqrt{a_l \gamma}), \tag{A.1}$$

where A_l and a_l are constants given in Table 5.1.

The average BER in a specific SNR region of $[\gamma_n, \gamma_{n+1}]$ can then be computed as follows:

$$P_{n,QAM} = \int_{\gamma_n}^{\gamma_{n+1}} p_{m_n,QAM}(\gamma) p_{\gamma_{sb}}(\gamma) d\gamma, \tag{A.2}$$

for an i.i.d Rayleigh fading for the cooperative network

$$p_{\gamma_{sb}}(\gamma) = \frac{\beta_0}{\bar{\gamma}_{s,d}} e^{-\frac{\gamma}{\bar{\gamma}_{s,d}}} + \sum_{i=1}^{m} \frac{\beta_i (0.5\bar{\gamma})^{-i}}{(i-1)!} \gamma^{i-1} e^{-\frac{\gamma}{(0.5\bar{\gamma})}}. \tag{A.3}$$

Substituting in (A.1) and (A.3) into (A.2), the n-th mode BER is given by

$$P_{n,QAM} = \int_{\gamma_n}^{\gamma_{n+1}} \sum_l A_l Q(\sqrt{a_l\gamma}) \left\{ \frac{\beta_0}{\bar{\gamma}_{s,d}} e^{-\frac{\gamma}{\bar{\gamma}_{s,d}}} + \sum_{i=1}^{m} \frac{\beta_i (0.5\bar{\gamma})^{-i}}{(i-1)!} \gamma^{i-1} e^{-\frac{\gamma}{(0.5\bar{\gamma})}} \right\} d\gamma \quad \text{(A.4)}$$

$$= \frac{\beta_0}{\bar{\gamma}_{s,d}} \sum_l A_l \int_{\gamma_n}^{\gamma_{n+1}} Q(\sqrt{a_l\gamma}) e^{-\frac{\gamma}{\bar{\gamma}_{s,d}}} d\gamma \quad \text{(A.5)}$$

$$+ \sum_l A_l \sum_{i=1}^{m} \frac{\beta_i (0.5\bar{\gamma})^{-i}}{(i-1)!} \int_{\gamma_n}^{\gamma_{n+1}} Q(\sqrt{a_l\gamma}) \gamma^{i-1} e^{-\frac{\gamma}{(0.5\bar{\gamma})}} d\gamma.$$

Eq. (A.5) can be solved as follows. First defining

$$I_i = \int_c^d Q(\sqrt{a_l\gamma}) \gamma^{i-1} e^{-\beta\gamma} d\gamma \quad \text{(A.6)}$$

$$= \int_c^d Q(\sqrt{a_l\gamma}) dF(\gamma) \quad \text{(A.7)}$$

$$= Q(\sqrt{a_l\gamma}) F(\gamma)\Big|_c^d - \int_c^d F(\gamma) \frac{d}{d\gamma} Q(\sqrt{a_l\gamma}) \quad \text{(A.8)}$$

where integration by parts is used in the step from (A.7) to (A.8) and $dF(\gamma) = \gamma^{i-1} e^{-\beta\gamma} d\gamma$.

Firstly, the CDF is give by

$$F(\gamma) = \int_0^\gamma dF(x) = \int_0^\gamma x^{i-1} e^{-\beta x} dx \quad \text{(A.9)}$$

$$= \beta^{-i} \int_0^{\beta\gamma} t^{i-1} e^{-t} dt = \beta^{-i} \gamma_{func}(i, \beta\gamma) \quad \text{(A.10)}$$

$$= \beta^{-i}(i-1)! \left[1 - e^{-\beta\gamma} \sum_{r=0}^{i-1} \frac{(\beta\gamma)^r}{r!} \right] \quad \text{(A.11)}$$

where, $\gamma_{func}(\alpha, x)$ is defined in [17, (8.350.1 & 8.352.1)] as

$$\gamma_{func}(\alpha, x) = \int_0^x t^{\alpha-1} e^{-t} dt \quad \text{(A.12)}$$

$$= (\alpha-1)! \left[1 - e^{-x} \sum_{r=0}^{\alpha-1} \frac{x^r}{r!} \right]; \text{for integer } \alpha = 1, 2, .. \quad \text{(A.13)}$$

Secondly, using the definition

$$Q(x) = \frac{1}{\sqrt{2\pi}} \int_x^\infty \exp(-\lambda^2/2) d\lambda, \quad \text{(A.14)}$$

the derivative can be given by

$$\frac{d}{dx}Q(x) = \frac{-\exp(-x^2/2)}{\sqrt{2\pi}}. \tag{A.15}$$

When $x = \sqrt{a_l\gamma} => dx = \frac{\sqrt{a_l}}{2}\gamma^{-0.5}d\gamma$. Getting,

$$\frac{d}{d\gamma}Q(\sqrt{a_l\gamma}) = -\frac{1}{2}\sqrt{\frac{a_l}{2\pi}}\gamma^{-0.5}\exp(-a_l\gamma/2). \tag{A.16}$$

By substituting (A.16) and (A.13) into (A.8), I_i can be written as,

$$\begin{aligned} I_i &= Q(\sqrt{a_l\gamma})\beta^{-i}(i-1)!\left[1 - e^{-\beta\gamma}\sum_{r=0}^{i-1}\frac{(\beta\gamma)^r}{r!}\right]\Big|_c^d \qquad \text{(A.17)} \\ &\quad + \frac{1}{2}\sqrt{\frac{a_l}{2\pi}}\beta^{-i}(i-1)!\int_c^d\left[1 - e^{-\beta\gamma}\sum_{r=0}^{i-1}\frac{(\beta\gamma)^r}{r!}\right]\gamma^{-0.5}\exp(-a_l\gamma/2)d\gamma. \end{aligned}$$

Now taking a look at the following,

$$\begin{aligned} &\textstyle\int_c^d\left[1 - e^{-\beta\gamma}\sum_{r=0}^{i-1}\frac{(\beta\gamma)^r}{r!}\right]\gamma^{-0.5}\exp(-a_l\gamma/2)d\gamma \\ &= \textstyle\int_c^d\gamma^{-0.5}\exp(-a_l\gamma/2)d\gamma - \int_c^d\exp(-\gamma(a_l/2+\beta))\sum_{r=0}^{i-1}\frac{\beta^r\gamma^{r-0.5}}{r!}d\gamma. \end{aligned} \tag{A.18}$$

Furthermore, looking at

$$\begin{aligned} \int_c^d\gamma^{r-0.5}\exp(-K\gamma)d\gamma &= K^{-r-0.5}\int_{cK}^{dK}t^{r-0.5}\exp(-t)dt \qquad \text{(A.19)} \\ &= -K^{-r-0.5}\Gamma(r+0.5, K\gamma)\Big|_c^d, \qquad \text{(A.20)} \end{aligned}$$

where the incomplete gamma function can be written as [17, (8.350.2)]

$$\Gamma(\alpha, x) = \int_x^\infty e^{-t}t^{\alpha-1}dt, \tag{A.21}$$

and (A.18) can then be written as

$$= -(\frac{a_l}{2})^{-0.5}\Gamma(0.5, \frac{\gamma a_l}{2})\Big|_c^d + \sum_{r=0}^{i-1}\frac{\beta^r}{r!}(a_l/2+\beta)^{-r-0.5}\Gamma(r+0.5, (a_l/2+\beta)\gamma)\Big|_c^d. \tag{A.22}$$

Finally, I_i can be written in closed form as,

$$
\begin{aligned}
I_i &= Q(\sqrt{a_l\gamma})\beta^{-i}(i-1)!\left[1-e^{-\beta\gamma}\sum_{r=0}^{i-1}\frac{(\beta\gamma)^r}{r!}\right]\Bigg|_c^d \\
&\quad -\frac{1}{2}\beta^{-i}(i-1)!\Bigg\{(\pi)^{-0.5}\Gamma(0.5,\frac{\gamma a_l}{2})\Big|_c^d \\
&\quad -\sqrt{\frac{a_l}{2\pi}}\sum_{r=0}^{i-1}\frac{\beta^r}{r!}(a_l/2+\beta)^{-r-0.5}\Gamma(r+0.5,(a_l/2+\beta)\gamma)\Big|_c^d\Bigg\}.
\end{aligned}
\tag{A.23}
$$

Also it is interesting to know I_1, given by

$$
\begin{aligned}
I_1 &= Q(\sqrt{a_l\gamma})\beta^{-1}\left[1-e^{-\beta\gamma}\right]\Big|_c^d \\
&\quad -\frac{1}{2}\beta^{-1}\Bigg\{(\pi)^{-0.5}\Gamma(0.5,\frac{\gamma a_l}{2})\Big|_c^d \\
&\quad -\sqrt{\frac{a_l}{2\pi}}(a_l/2+\beta)^{-0.5}\Gamma(0.5,(a_l/2+\beta)\gamma)\Big|_c^d\Bigg\}.
\end{aligned}
\tag{A.24}
$$

Lastly, the average BER of (A.5) can be written as follows by substituting in I_1 and I_i,

$$
\begin{aligned}
P_{n,QAM} &= \beta_0\sum_l A_l\Bigg[Q(\sqrt{a_l\gamma})\left[1-e^{-\frac{\gamma}{\bar{\gamma}_{s,d}}}\right]\Big|_{\gamma_n}^{\gamma_{n+1}} \\
&\quad -\frac{1}{2}\Bigg\{(\pi)^{-0.5}\Gamma(0.5,\frac{\gamma a_l}{2})\Big|_{\gamma_n}^{\gamma_{n+1}} \\
&\quad -\sqrt{\frac{a_l}{2\pi}}(a_l/2+\bar{\gamma}_{s,d}^{-1})^{-0.5}\Gamma(0.5,(a_l/2+\bar{\gamma}_{s,d}^{-1})\gamma)\Big|_{\gamma_n}^{\gamma_{n+1}}\Bigg\}\Bigg] \\
&\quad +\sum_l A_l\sum_{i=1}^{m}\beta_i\Bigg[Q(\sqrt{a_l\gamma})\left(1-e^{-\frac{\gamma}{(0.5\bar{\gamma})}}\sum_{r=0}^{i-1}\frac{(2\gamma/\bar{\gamma})^r}{r!}\right)\Bigg|_{\gamma_n}^{\gamma_{n+1}} \\
&\quad -\frac{1}{2}\Bigg\{(\pi)^{-0.5}\Gamma(0.5,\frac{\gamma a_l}{2})\Big|_{\gamma_n}^{\gamma_{n+1}} \\
&\quad -\sqrt{\frac{a_l}{2\pi}}\sum_{r=0}^{i-1}\frac{(0.5\bar{\gamma})^{-r}}{r!}(a_l/2+2/\bar{\gamma})^{-r-0.5}\Gamma(r+0.5,(a_l/2+2/\bar{\gamma})\gamma)\Big|_{\gamma_n}^{\gamma_{n+1}}\Bigg\}\Bigg].
\end{aligned}
\tag{A.25}
$$

A.2 The Case of Non-I.I.D. Fading Channels

In a similar fashion as the i.i.d. case, and by making use of the non-i.i.d. pdf,

$$p_{\gamma_{ab}}(\gamma) = \frac{\widehat{\beta}_0}{\bar{\gamma}_{s,d}} e^{-\frac{\gamma}{\bar{\gamma}_{s,d}}} + \sum_{i=1}^{m} \frac{\widehat{\beta}_i}{\tau_i} e^{-\frac{\gamma}{\tau_i}}. \tag{A.26}$$

and substituting in (A.1) and (A.26) into (A.2) getting the n-th mode BER as,

$$P_{n,QAM} = \int_{\gamma_n}^{\gamma_{n+1}} \sum_{l} A_l Q(\sqrt{a_l \gamma}) \left\{ \frac{\widehat{\beta}_0}{\bar{\gamma}_{s,d}} e^{-\frac{\gamma}{\bar{\gamma}_{s,d}}} + \sum_{i=1}^{m} \frac{\widehat{\beta}_i}{\tau_i} e^{-\frac{\gamma}{\tau_i}} \right\} d\gamma. \tag{A.27}$$

Equation (A.27) can be rearranged as

$$\begin{aligned} P_{n,QAM} &= \frac{\widehat{\beta}_0}{\bar{\gamma}_{s,d}} \sum_{l} A_l \int_{\gamma_n}^{\gamma_{n+1}} Q(\sqrt{a_l \gamma}) e^{-\frac{\gamma}{\bar{\gamma}_{s,d}}} d\gamma \\ &\quad + \sum_{l} A_l \sum_{i=1}^{m} \frac{\widehat{\beta}_i}{\tau_i} \int_{\gamma_n}^{\gamma_{n+1}} Q(\sqrt{a_l \gamma}) e^{-\frac{\gamma}{\tau_i}} d\gamma. \end{aligned} \tag{A.28}$$

Substituting in I_1 (A.24) into (A.28), it can be found that

$$\begin{aligned} P_{n,QAM} &= \widehat{\beta}_0 \sum_{l} A_l \left[Q(\sqrt{a_l \gamma}) \left[1 - e^{-\frac{\gamma}{\bar{\gamma}_{s,d}}} \right] \Big|_{\gamma_n}^{\gamma_{n+1}} \right. \\ &\quad - \frac{1}{2} \left\{ (\pi)^{-0.5} \Gamma(0.5, \frac{\gamma a_l}{2}) \Big|_{\gamma_n}^{\gamma_{n+1}} \right. \\ &\quad \left. \left. - \sqrt{\frac{a_l}{2\pi}} (a_l/2 + \bar{\gamma}_{s,d}^{-1})^{-0.5} \Gamma(0.5, (a_l/2 + \bar{\gamma}_{s,d}^{-1})\gamma) \Big|_{\gamma_n}^{\gamma_{n+1}} \right\} \right] \\ &\quad + \sum_{l} A_l \sum_{i=1}^{m} \widehat{\beta}_i \left[Q(\sqrt{a_l \gamma}) \left[1 - e^{-\frac{\gamma}{\tau_i}} \right] \Big|_{\gamma_n}^{\gamma_{n+1}} \right. \\ &\quad - \frac{1}{2} \left\{ (\pi)^{-0.5} \Gamma(0.5, \frac{\gamma a_l}{2}) \Big|_{\gamma_n}^{\gamma_{n+1}} \right. \\ &\quad \left. \left. \left. - \sqrt{\frac{a_l}{2\pi}} (a_l/2 + \tau_i^{-1})^{-0.5} \Gamma(0.5, (a_l/2 + \tau_i^{-1})\gamma) \Big|_{\gamma_n}^{\gamma_{n+1}} \right\} \right]. \end{aligned} \tag{A.29}$$

References

[1] Mohamed-Slim Alouini and Andrea J. Goldsmith. Capacity of Rayleigh fading channels under different adaptive transmission and diversity-combining techniques. *IEEE Trans. Veh. Technol.*, 48:1165–1181, July 1999.

[2] Mohamed-Slim Alouini and Andrea J. Goldsmith. Adaptive modulation over Nakagami fading channels. *Wireless Personal Comm.*, 13:119–143, 2000.

[3] Paul A. Anghel and Mostafa Kaveh. Exact symbol error probability of a cooperative network in a Rayleigh-fading environment. *IEEE Trans. Wireless Commun.*, 3:1416–1421, September 2004.

[4] A. S. Avestimehr and D. N. C. Tse. Outage capacity of the fading relay channel in the low-SNR regime. *IEEE Trans. Inform. Theory*, 53(4):1401–1415, April 2007.

[5] N. C. Beaulieu and J. Hu. A closed-form expression for the outage probability of decode-and-forward relaying in dissimilar Rayleigh fading channels. *IEEE Commun. Letters*, 10(12):813–815, December 2006.

[6] O. Canpolat, M. Uysal, and M. M. Fareed. Analysis and design of distributed space-time trellis codes with amplify-and-forward relaying. *IEEE Trans. Veh. Technol.*, 56:1649–1660, July 2007.

[7] J. Cavers. Variable-rate transmission for rayleigh fading channels. *Communications, IEEE Transactions on [legacy, pre - 1988]*, 20(1):15–22, February 1972.

[8] Byoungjo Choi and L. Hanzo. Optimum mode-switching-assisted constant-power single- and multicarrier adaptive modulation. *IEEE Trans. Veh. Technol.*, 52(3):536–560, May 2003.

[9] T. Cover and A.E. Gamal. Capacity theorems for the relay channel. *IEEE Trans. Inform. Theory*, 25(5):572–584, Sep 1979.

[10] A. Doufexi, S. Armour, M. Butler, A. Nix, D. Bull, J. McGeehan, and P. Karlsson. A comparison of the hiperlan/2 and ieee 802.11a wireless lan standards. *Communications Magazine, IEEE*, 40(5):172–180, May 2002.

[11] Jr. Forney, G., R. Gallager, G. Lang, F. Longstaff, and S. Qureshi. Efficient modulation for band-limited channels. *IEEE J. Select. Areas in Commun.*, 2(5):632–647, September 1984.

[12] H. P. Frank and Fitzek Katz. *Cooperation in Wireless Networks: Principles and Applications: Real Egoistic Behavior Is to Cooperate!* Springer-Verlag New York, Inc., Secaucus, NJ, USA, 2006.

[13] A. Furuskar, S. Mazur, F. Muller, and H. Olofsson. EDGE: enhanced data rates for GSM and TDMA/136 evolution. *IEEE [see also IEEE Wireless Communications] Personal Communications*, 6(3):56–66, June 1999.

[14] Andrea Goldsmith. *Wireless Communications*. Cambridge University Press, New York, NY, USA, 2005.

[15] Andrea J. Goldsmith and Soon-Ghee Chua. Variable-rate variable-power MQAM for fading channels. *IEEE Trans. Commun.*, 45:1218–1230, October 1997.

[16] Andrea J. Goldsmith and Pravin P. Varaiya. Capacity of fading channels with channel side information. *IEEE Trans. Inform. Theory*, 43:1986–1992, November 1997.

[17] I.S. Gradshteyn and I.M. Ryzhik. *Table of Integrals, Series, and Products, Sixth Edition*. Academic Press, 2000.

[18] D. Gunduz and E. Erkip. Opportunistic cooperation by dynamic resource allocation. *IEEE Trans. Wireless Commun.*, 6(4):1446–1454, April 2007.

[19] Mazen O. Hasna and Mohamed-Slim Alouini. End-to-end performance of transmission system with relays over Rayleigh-fading channels. *IEEE Trans. Wireless Commun.*, 2:1126–1131, November 2003.

[20] J. Hayes. Adaptive feedback communications. *Communications, IEEE Transactions on [legacy, pre - 1988]*, 16(1):29–34, February 1968.

[21] A. Host-Madsen and J. Zhang. Capacity bounds and power allocation for wireless relay channels. *IEEE Trans. Inform. Theory*, 51(6):2020–2040, June 2005.

[22] K. S. Hwang, Y. Ko, and M.-S. Alouini. Performance analysis of opportunistic incremental relaying with adaptive modulation. In *Proc. IEEE International Symposium on Wireless Pervasive Computing 2008*, May 2008.

[23] Salama Ikki and Mohamed H. Ahmed. Performance analysis of cooperative diversity wireless networks over Nakagami-m fading channel. *IEEE Commun. Letters*, 11:334–336, July 2007.

[24] O. Kaya and S. Ulukus. Power control for fading multiple access channels with user cooperation. In *Wireless Networks, Communications and Mobile Computing, 2005 International Conference on*, volume 2, pages 1443–1448, June 2005.

[25] Y. Ko and C. Tepedelenlioglu. Orthogonal space-time block coded rate-adaptive modulation with outdated feedback. *IEEE Trans. on Wireless Commun.*, 5(2):290–295, February 2006.

[26] J. Nicholas Laneman, David N. C. Tse, and Gregory W. Wornell. Cooperative diversity in wireless networks: Efficient protocols and outage behavior. *IEEE Trans. Inform. Theory*, 50:3062–3080, December 2004.

[27] J. Nicholas Laneman and Gregory W. Wornell. Distributed space-time-coded protocols for exploiting cooperative diversity in wireless networks. *IEEE Trans. Inform. Theory*, 49:2415–2425, November 2003.

[28] Long Le and E. Hossain. An analytical model for ARQ cooperative diversity in multi-hop wireless networks. *to appear IEEE Trans. on Wireless Commun.*

[29] M.J. Lee, Jianliang Zheng, Young-Bae Ko, and D.M. Shrestha. Emerging standards for wireless mesh technology. *Wireless Communications, IEEE [see also IEEE Personal Communications]*, 13(2):56–63, April 2006.

[30] Yingbin Liang and V. V. Veeravalli. Resource allocation for wireless relay channels. In *Signals, Systems and Computers, 2004. Conference Record of the Thirty-Eighth Asilomar Conference on*, volume 2, pages 1902–1906, November 2004.

[31] Rajan K. Mallik, Moe Z. Win, Mohamed-Slim Alouini, and Andrea J. Goldsmith. Channel capacity of adaptive transmission with maximal ratio combining in correlated Rayleigh fading. *IEEE Trans. Wireless Commun.*, 3:1124–1133, July 2004.

[32] D. S. Michalopoulos and G. K. Karagiannidis. PHY-layer fairness in amplify and forward cooperative diversity systems. *IEEE Trans. Wireless Commun.*, 7(3):1073–1082, March 2008.

[33] S. Nanda, K. Balachandran, and S. Kumar. Adaptation techniques in wireless packet data services. *IEEE Communications Magazine*, 38(1):54–64, January 2000.

[34] T. Nechiporenko, Prasanna Kalansuriya, and Chintha Tellambura. Performance of optimum switching adaptive m-qam for amplify-and-forward relays. *submitted to IEEE Trans. on Veh. Technol.*

[35] T. Nechiporenko, Khoa T. Phan, Chintha Tellambura, and Ha H. Nguyen. Performance analysis of adaptive m-qam for rayleigh fading cooperative systems. In *Proc. IEEE International Conference on Communications (ICC)*, pages 3393–3399, May 2008.

[36] T. Nechiporenko, Khoa T. Phan, Chintha Tellambura, and Ha H. Nguyen. Capacity of Rayleigh fading cooperative systems under adaptive transmission. *to appear in IEEE Trans. on Wireless Commun.*, available online at http://www.ece.ualberta.ca/~nechipor.

[37] Chris T. K. Ng and Andrea J. Goldsmith. The impact of CSI and power allocation on relay channel capacity and cooperation strategies, http://www.citebase.org/abstract?id=oai:arXiv.org:cs/0701116, 2007.

[38] S. Otsuki, S. Sampei, and N. Morinaga. Square-QAM adaptive modulation/TDMA/TDD systems using modulation level estimation with walsh function. *Electronics Letters*, 31:169–171, February 1995.

[39] J. Peng and L. Cheng. Revisiting carrier sense multiple access with collision avoidance (CSMA/CA). In *Information Sciences and Systems, 2006 40th Annual Conference on*, pages 1236–1241, Princeton, NJ, March 2006.

[40] A. Sendonaris, E. Erkip, and B. Aazhang. User cooperation diversity part I: system description. *IEEE Trans. Commun.*, 51:1927–1938, November 2003.

[41] A. Sendonaris, E. Erkip, and B. Aazhang. User cooperation diversity part II: implementation aspects and performance analysis. *IEEE Trans. Commun.*, 51:1939–1948, November 2003.

[42] V. Stankovic, A. Host-Madsen, and Zixiang Xiong. Cooperative diversity for wireless ad hoc networks. *IEEE Signal Processing Magazine*, 23(5):37–49, September 2006.

[43] H. A. Suraweera, P. J. Smith, and J. Armstrong. Outage probability of cooperative relay networks in Nakagami-m fading channels. *IEEE Commun. Letters*, 10(12):834–836, December 2006.

[44] David Tse and Pramod Viswanath. *Fundamentals of wireless communication*. Cambridge University Press, New York, NY, USA, 2005.

[45] B. Vucetic. An adaptive coding scheme for time-varying channels. *IEEE Transactions on Communications*, 39(5):653–663, May 1991.

[46] W. T. Webb and R. Steele. Variable rate QAM for mobile radio. *IEEE Transactions on Communications*, 43(7):2223–2230, July 1995.

[47] S. Yiu, R. Schober, and L. Lampe. Distributed space-time block coding. *IEEE Trans. Commun.*, 54(7):1195–1206, July 2006.

[48] Y. Zhao, R. Adve, and T. J. Lim. Improving amplify-and-forward relay networks: optimal power allocation versus selection. *IEEE Trans. Wireless Commun.*, 6(8):3114–3123, August 2007.

[49] Zhendong Zhou, B. Vucetic, M. Dohler, and Yonghui Li. MIMO systems with adaptive modulation. *IEEE Transactions on Vehicular Technology*, 54(5):1828–1842, September 2005.